Master's thesis

NTNU
Norwegian University of Science and Technology
Faculty of Engineering
Department of Civil and Environmental Engineering

Sabin Bhandari

2D Numerical Simulation of Sediment Flushing in a Hydropower Reservoir

Master's thesis in Hydropower Development
Supervisor: Nils Rüther
Co-supervisor: Behnam Balouchi and Hans Bihs
July 2021

NTNU
Norwegian University of
Science and Technology

Sabin Bhandari

2D Numerical Simulation of Sediment Flushing in a Hydropower Reservoir

Master's thesis in Hydropower Development
Supervisor: Nils Rüther
Co-supervisor: Behnam Balouchi and Hans Bihs
July 2021

Norwegian University of Science and Technology
Faculty of Engineering
Department of Civil and Environmental Engineering

NTNU
Norwegian University of
Science and Technology

Acknowledgement

I would like convey my wholehearted gratitude to Professor Nils Rüther for his valuable support and advices. I am highly indebted to my co- supervisor Behnam Balouchi (Postdoctoral researcher, NTNU) and Adjunct Associate Professor Hans Bihs for their effortless dedication, support, regular guidance and encouragement throughout the working period. I would also like to acknowledge Diwash Lal Maskey (PhD candidate, NTNU) for his valuable time on providing necessary suggestions and documents.

I am very grateful to my loving family who has always supported and inspired me with their unconditional love. A special thanks to my friends for motivating and boosting which help me to keep up and channelize my dedication on work.

Abstract

The Binga Hydropower Plant has been facing problems related to sedimentation. After completion, reservoir was filled up rapidly with sediment due to lack of sediment management facility and the underestimation of sediment load from the catchment area. The sediment delta is approaching near the dam which have potential to seriously damage the hydraulic structure and plant's units. Due to sedimentation rate of storage loss increases so, flushing of sediment out of reservoir is crucial to reduce the possible threat imposed by delta and to operate Binga as a run-of river project. So, the primary idea of this topic is to investigate the technical possibilities to use a 2D numerical model to flush sediment out of reservoir during draw down operation.

A 2D numerical model with structured immersed boundary condition to generate grid from topographic data was used for simulation. The numerical model of hydrodynamic simulation(scale of 1:66.67, as implemented for physical model) is carried out which first calibrated and validated against the measured inflow velocity profile and water surface elevation at different control points in the physical model. The model is simulated using different range of global roughness value. Based on the flow pattern, velocity distribution profile global roughness of 0.166 is chosen for further simulation analysis.

Sediment simulation is carried out using average sediment size d_{50} for two different constant discharge conditions i.e.500 m^3/sec and 1000 m^3/sec to observe the scour and deposition pattern.The time development of deposition and erosion is observed. Conservative finite-difference framework on structured-staggered grid was used to descretize RANS(Reynolds-Averaged Stokes (RANS) equation with fifth-order WENO (weighted essentially non-oscillatory) scheme and third-order Runge-Kutta explicit scheme was used for time discretization. The location of free surface is presented using level set method. Domain decomposition coupled with MPI library is used to achieve the parallelization of numerical model. The complex geometry in numerical model area handled with an immersed boundary method based on ghost cell extrapolation.

In the final stage, the scouring and deposition pattern is modelled for both discharges. The numerical result is compared with the data obtained from the experiment conducted in Norsk Hydroteknisk Laboratorium, Norwegian University of Science and Technology (NTNU). The comparison is done on the basis of change in bed level by computing the raster map of both physical and simulated topographic data. The validation is also done by computing the change in volume of bed in the areas where scouring and deposition process was occurred on the basis of raster map using Arcgis.

In context of flushing with 500 m^3/sec, the scouring and deposition pattern and the change in bed volume is in well agreement with physical model. While in 1000 m^3/sec, the simulated results in terms of deposition and scouring pattern is different and volume is overestimated as compared to physical model.

Contents

List of Figures

List of Tables

1 Introduction

1.1 Background

Construction of dam provides the storage of water along with the safe retention forming the reservoir. Based on the purpose of reservoirs, it can be classified into different groups like hydroelectric power generation, flood control, irrigation, river regulation, water supply, and so on (Novák et al., 2017). Numerous dams are constructed to date. According to ICOLD, 58,173 dams are registered. Among which 49% are single-purpose dam and approximately 18% are multipurpose. In case of the multipurpose dam around 24% are used for Irrigation purposes, 20% for flood control. These dams equally contribute to electricity generation and flood control i.e. 16%. Regarding single purpose dam, almost half of them are used for irrigation purpose, 21% for hydropower,21% and 9% for water supply and flood control respectively and almost 11% for fish farming, navigation, and recreation purposes (icold, 2021).

Directly or indirectly every development activity has both negative and positive impacts on the purposed site. Similarly, the construction of a large reservoir contributed to the optimum utilization of water resources, while on other hand it blocks the transport of sediment to downstream. Since the construction of the dam started, importance was not given to sedimentation and its effects. The silting process was not taken into consideration during the design of dams and the sediment management facilities like a bottom outlet for flushing were excluded in some of the large reservoirs. This leads to sedimentation which gradually decreases the reservoir storage capacity and finally kills the reservoir system (Mohammad et al., 2020).

More than 100 billion metric tons of sediment, which contributes 26% of the global sediment release is trapped in the reservoirs (Syvitski et al., 2005). The river Basins like Nile and Colorado theoretically trap all the sediment in reservoir (Vörösmarty et al., 2003). Lack of sustainable management strategies lowers rate of construction of a reservoir while the ongoing sedimentation in existing reservoir decline the reservoir storage volume. If the population growth is considered, the per capita storage is decreasing rapidly globally (Annandale, 2013). The decreasing reservoir capacity has an adverse impact on the availability for irrigation, water supplies for households along with hydropower, navigation, flood control, and recreational purposes. The problems due to sedimentation are not only limited to the reservoir area, it also affects the downstream area by retaining the sediment loads resulting in loss of habitat, bank erosion which plays a vital role in maintaining the channel morphology(Kondolf, 1997).

A proper sediment management plan is essential and should be strictly implemented for the sustainable utilization of reservoirs. Sediment management plan contributes in balancing sediment inflow and outflow, synchronizing natural sediment release to the downstream area, increase long-term storage capacity, and other benefits with the minimum impacts on the environment (Morris, 2020).

Among the different strategies for sediment management, Sediment Sluicing by Reservoir Drawdown is one. Sediment sluicing is the process of increasing sediment release through the reservoir by lowering pool level during the high flood. This process decreases retention time increasing flow velocity which brings sediment in motion reducing the probability of sediment being trapped in the reservoir. It mainly targets maintaining the balance between the sediment inflow and at the downstream. Taking hydrology and site conditions, sluicing can be carried out as seasonal or based on events where the reservoir is operated on the basis of real-time hydrologic modeling and reporting gages (Morris, 2020). Regarding the effectiveness of sluicing, a small reservoir capturing only a fraction of annual runoff volume and with a low-level outlet of high release capacity. For E.g. concrete dams in japan are retrofitted with deeper gates for the sediment sluicing (Sumi et al., 2015). Sluicing is suitable in those projects with an elongated, nearly circular reservoir having inefficient geometry for sediment delivery and limited drawdown facility (Lee and Foster, 2013). Sediment Sluicing by drawdown represents a less expensive method to reduce the sediment deposit which must be eventually removed by more costly operations like dredging. Even though sediment sluicing by drawdown is not considered in earlier years, it can be attractive later in the reservoir when its storage capacity shrinks. As the sediment release to downstream during the flood events does not have a high concentration of suspended sediment compared to emptying and flushing of the reservoir, it is important to evaluate and maximize the efficiency of sediment sluicing by the drawdown method. Flushing is very costly considering the operational point of view so it is crucial to know the efficiency in an earlier stage which helps to operate the reservoir in optimum level. So to investigate the efficiency of flushing considering different discharges, a test case of Binga Hydropower Plant in the Philippines has been considered in this study.

1.2 Master Thesis Work

The purpose of this thesis is to study the flushing of sediment by the drawdown method in Binga HPP reservoir using a two-dimensional numerical model, REEF3D: SFLOW. The main objectives of this study are:

1. Literature review on drawdown sediment flushing in terms of application range and efficiency
2. Setting up the grid for the study case in a 2D hydrodynamic model
3. Document the flow situation for 1000 m3/s and compare with the data of the physical model
4. Run the numerical model for the flushing of 500 m3/s and 1000 m3/s and compare with the data obtained by the physical model
5. Based on the results suggest a strategy for the optimal flushing operation with respect to discharge
6. Discussion of the results
7. Conclusions
8. Proposals for future work

2 Literature Review

2.1 Reservoir Sedimentation

Dams were constructed to store water, flood prevention, irrigation, and water supply also. Besides, they have been mainly used for the generation of power. Different problems related to the dam structure, water management, reservoir storage, and power generation have been rising along with time. The trapping of sedimentation upstream of a dam can be considered as the main reason for the above-mentioned problems (Tigrek and Aras, 2011). The sedimentation process depends on different factors like basin characteristics, hydrology of the catchments, and the erosion of the surrounding areas. Sedimentation in reservoir results in reservoir capacity loss along with negative influences in the upstream and downstream area. Globally, the annual loss rates relative to installed capacity are generally estimated to range between 0.5 and 1 % (Mahmood, 1987). Loss of storage capacity is one of the many sedimentation problems. With the development of hydropower and water management projects, sedimentation affects different aspects like technical, economic, and ecological. Reservoir sedimentation considerably decreases the subsidies obtained from power generation, irrigation, water supply, and flood control. So maintaining the storage capacity by developing new projects is not feasible concerning sites, economical and financial.

Sustainable development of hydropower projects can be one of the alternatives for those dams or reservoirs which are meant to be long-term and for multipurpose use (Morris and Fan, 1998). Sustainable development of hydropower consists of diverse techniques for the management of sediment in reservoirs including the forecasting of erosion rate, transport, and siltation. Not only this, evaluation of an approach for prevention of sediment flow and deposition, and procedure to remove deposited sediment with reservoir operation plays a vital role in sediment management (Tigrek and Aras, 2011).

2.2 Sediment Deposition in Reservoir

Sediment is a naturally occurring fragment of rocks and minerals formed from chemical and mechanical activity which results in a change in properties, decay, detached and removed from any part of the earth surface, and eventually disintegrate into soil (Morris and Fan, 1998). In a river system, these sediments can be classified into different groups like Bedload, Wash load, and Suspended load. Bedload refers to those sediments which move close to the bed by rolling, saltation, and sliding and remain in bed. The suspended sediment which does not touch the bed is called as Wash load. And suspended sediments cover all particles which are transported by the flow in suspension and travel with a velocity approximately equal to flow (Lysne et al., 2003). Sediment transport is a natural phenomenon and a complex process. It depends on the different factors like river discharge, catchment properties, sediment yield, concentration, sediment density, turbulence, and forces on sediment. Sediments with higher density tend to remain stable in river bed in which gravity also provides stabilizing force. The river velocity and turbulence tend to move the sediments either in suspension or as bedload. River basins are highly affected by human activities like construction, mines

exploration, and agriculture with the consequences of land erosion and contribution to the sediment transport in the reservoir. So, the natural river system itself tries to maintain the hydraulic sedimentological equilibrium (Lysne et al., 2003). The siltation process starts when the tributary reach and the river flow meets water impounded reservoir/reach because it fails to retains its sediment carrying capacity due to decrease inflow velocity. The delta formation took place at the entrance immediately after the deposition of coarse and bedload fraction of suspended load. Relatively fine sediment having lower settling velocity are driven deeper into the reservoir by stratified or non-stratified flow and the finest one to the dam structure with density currents. The sediment deposit pattern can be reflected in three processes: (1) transport of coarse sediment as bed load along topset of triangular-shaped delta, (2) transport of fines in turbid currents, and (3) transport of fines as non-stratifies flow. The depositional pattern depends on various factors like hydrologic conditions, reservoir geometry, and sediment grain size.

The longitudinal depositions zone can be categorized into three parts. (1) Topset beds refer to delta deposits of rapidly settling sediments. (2) Foreset deposits correspond the face of the delta accelerating into the reservoir. (3) Bottomset beds include fine sediment deposited by turbidity beyond the delta (Morris and Fan, 1998;Tigrek and Aras, 2011).

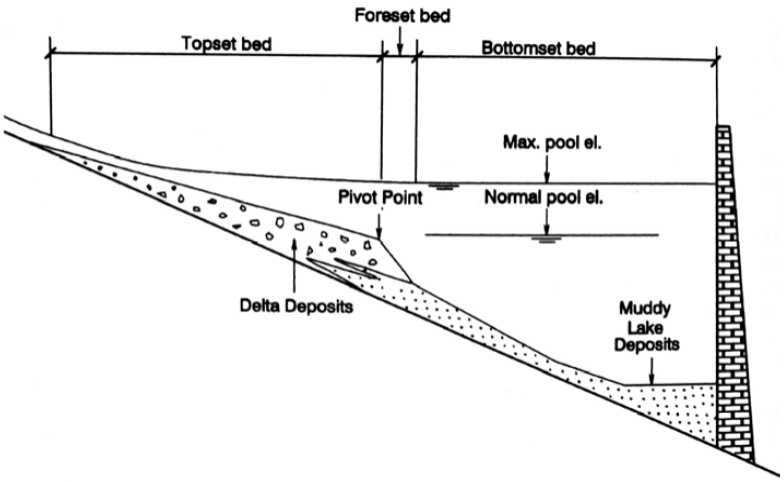

Figure 1: Generalized depositional zones in a reservoir (Morris and Fan, 1998)

2.3 Sediment problem in Reservoir

The sediment inflow and the outflow are approximately balanced in the natural river system which is termed as hydraulic sedimentological equilibrium (Lysne et al., 2003).But the construction of a dam definitely affects this equilibrium by the formation of a reservoir behind the dam, defined with very low flow velocity and sediment trapping efficiency of nearly 100 %. Sedimentation results in the loss of storage and ultimately eradicate the ability of flow regulation and other benefits such as water supply, flood control, hydropower, naviga-

tion, and environmental benefits which depend on the release from reservoir storage. It also reduces the life span of those structures (Morris and Fan, 1998).

Different types of sediment problems can be observed in both upstream and downstream of the dam, silting can hinder the advantages of diverted water. Sediment can block the intake and contribute to the abrasion of hydraulic machinery like turbines as a result of which efficiency decreases and maintenance cost increases. The cost for restoring/maintaining those structures can be estimated at US$ 13 billion per year (Annandale, 2013). Sedimentation reduces the active storage reducing both energy production and availability of water for water supply and irrigation. This problem will be in an extreme situation if countermeasure is not evaluated and implemented (Auel and Boes, 2011).

2.4 Sediment Management in Reservoir

Sediment management encompasses various methods which change the pool geometry, hydraulics, or both to move the sediment to the downstream to the dam in order to minimize the silting process (Morris and Fan, 1998). Some methods handle inflowing sediment while others try to evacuate siltation (Tigrek and Aras, 2011). The sediment load is time-dependent and also varies along the pool cross-section. The sediment Management technique helps to identify sediment-prone zone and manage it differently in order to reduce or counter sediment deposition. The management techniques vary from region to region although the problems are the same. It is because every pool/basin is characterized with different geology, geography, and climate. For example, dredging technique is mostly used in semi-arid regions like China. However, flushing procedures are used in north European countries (Tigrek and Aras, 2011). Some technique may involve the emptying of the reservoir which is different from flushing, which also includes reservoir emptying. The sediment management system either minimizes the deposition or removes the deposited sediment. Minimizing or balancing of deposition comes under sediment routing whereas flushing is used to remove the deposited one. The operational approach and the outcomes of reservoir drawdown and emptying under these two methods are different (Tigrek and Aras, 2011).

Sediment Management Strategies for the reservoir is classified into four parts. They are:

1. Reduce Sediment Yield
   - **(a)** Reduce Erosion
   - **(b)** Trap Sediment Upstream
2. Route Sediments
   - **(a)** Sediment Bypass
   - **(b)** Sediment Pass-Through

3. Remove Deposited Sediment
   - **(a)** Mechanical Removal
   - **(b)** Hydraulic Scour
4. Adaptive Strategies
   - **(a)** Redistribute Sediment
   - **(b)** Increase Storage
   - **(c)** Increase Operational Efficiency

An efficient method needs to be enforced collaboratively with both proactive and adaptive strategies depending on various factors like technical, environmental, hydrological, financial, climatic, and other conditions to manage the sediment for the sustainable use of the reservoir.

2.4.1 Sediment Pass-Through

This technique focuses on passing sediment through the reservoir by lowering water level during the high flow event. On the basis of the flow event, this technique is divided into the following categories:

1. Seasonal Drawdown
2. Flood Drawdown
3. Flood Drawdown by Rule Curve

2.4.1.1 Seasonal Drawdown

Any reservoir operated under the seasonal drawdown is emptied partially or fully during flood season. This type of drawdown is carried during a predetermined period every year. In case of partial drawdown, the reservoir is maintained at the lowest operating level during high flow events to decease the hydraulic retention time(increase inflow velocity) and reduce the sediment trapping. Efficiency is defined by the sediment transport capacity at downstream compared to the inflow sediment. Under ideal condition, sediment balance can be achieved if the reservoir is operated by using partial drawdown every year (Morris and Fan, 1998).

2.4.1.2 Flood drawdown

Long-term sediment equilibrium can be achieved when the sediment inflow and release are balanced in terms of sediment quantity and grain-size distribution. This can be achieved only in ideal condition because the coarse fraction of load continues to accumulate. Although if sediment equilibrium cannot be achieved, sediment pass-through can decline the cost, environmental impact, and frequency which are linked with other techniques like flushing, dredging. This method can help to extend the reservoir life where flushing facilities are

not provided like Binga HPP. Sediment release efficiency may vary widely in the drawdown process. if there is scour from the previously deposited sediment, the efficiency can exceed 100%. The duration of discharge plays a vital role in sediment release. For a specific discharge and flow duration, the inflow sediment smaller than a certain diameter can be passed through reservoir but for the larger sediment size the release rate will go on decreasing and the larger size load can be accumulated in the reservoir. So, the transport rate of those larger diameter grains can be increased by increasing flow velocity i.e.more drawdown.

Flood Drawdown can be controlled with the hydrograph prediction. Under this technique, the reservoir is drawdown to the low level before the flood event and pass the flood with refilling the reservoir from the hydrograph recession. For the application of this method, the inflow must be greater than the outflow discharge. Early drawdown can help to improve the efficiency of sediment pass through in those sites where velocities are too low to bring the deposited sediment into motion. Depending on the flood forecast, reservoir volume, and gate capacity, a more efficient drawdown can be carried during the flood event. To achieve maximum efficiency, the drawdown is done to its lowest operating level before the arrival of the flood wave and all the gates are opened considering the rating curve of the gate. This process is described below and presented in Fig.2.

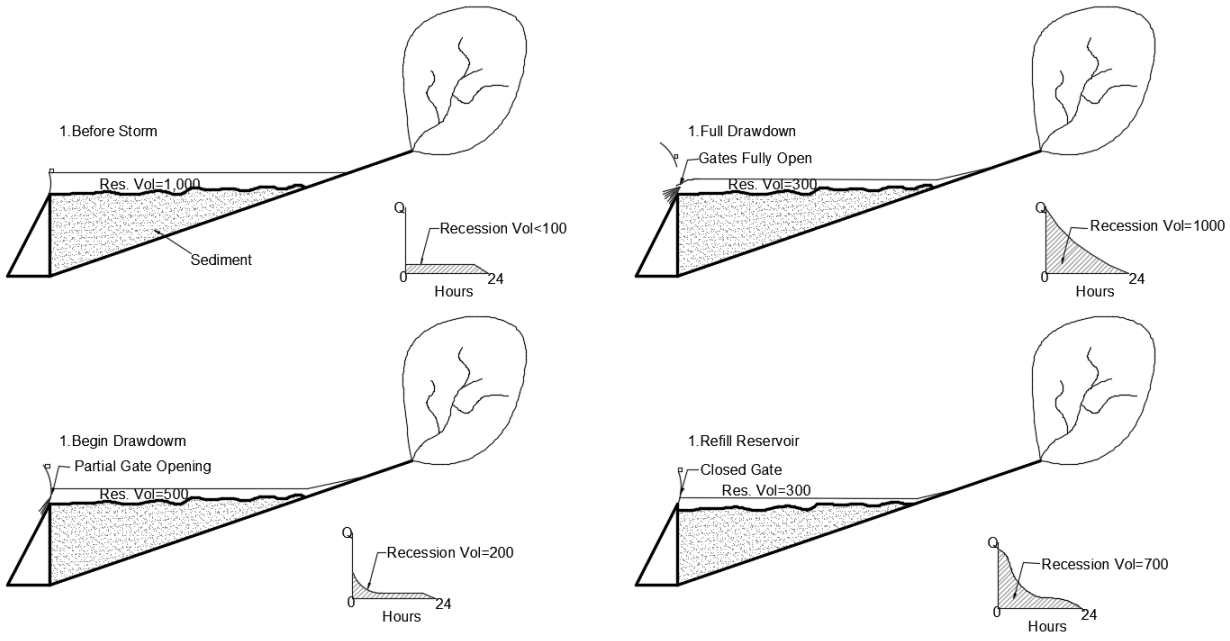

Figure 2: Operational sequence to pass suspended sediment, based of flood drawdown by hydrograph prediction [Redrawn after (Morris and Fan, 1998) for better readability]

1. Impounding:
   During the flood event, the reservoir is impounded as normal. Weather forecast is updated regularly to get information on meteorological conditions that can have a high runoff.

2. Lowering:
   When the high flow event begins, gates are opened to lower the pool up to the available minimum level so that reservoir can be still operated.
3. Full drawdown:
   Gates are fully opened to achieve the full drawdown generating the highest flow velocity regarding the specific discharge.
4. Refill: Reservoir storage volume and the hydrograph volume is monitored so that the refill of the reservoir can be done when that volume reduces to total reservoir volume.

2.4.1.3 Flood Drawdown by Rule Curve

For sediment management strategy, drawdown by rule curve can be implemented on those reservoirs which lack the bottom outlets for sediment flushing as in Binga HPP. During the flood event to pass the sediment downstream, this technique encompasses the lowering of water by operating gates as per the rule curve. Longer duration drawdown with lower level will contribute to a higher amount of sediment transport through impound reach.

2.5 Numerical Modeling

Sediment transport models can be numerically simulated in one, two, and three dimensional depending on the requirement of more reliable results. Two-dimensional and three-dimensional models require high computations time, data as compared to one-dimensional modeling (Molinas and Yang, 1986). The numerical theory implemented in solving the equations governing water and sediment is more stable and reliable and also provides good computational efficiency over two- and three-dimensional models (El kadi Abderrezzak and Paquier, 2009). The software like HEC-RAS, MIKE 11, and DAMBRK are used for one-dimensional simulations which offer the reliable result for unsteady flow and wave simulation on dam break(Lysne et al., 2003).

In two-dimensional models, the parameters are horizontally or vertically integrated. 2D sediment transport models are based on depth-integrated equations of continuity and motion(Chaudhary et al., 2019). In the 2D model, the profile adjustment and the prognosis of channel geometry are favorable for long-term simulation and also for the prediction of morphological changes(Ahn, 2012). Continuity and momentum equations that are laterally integrated are solved using laterally unified models(Smith and O'Connor, 1977). Some examples of 2D models to investigate sediment transport are MIKE 21 by DHI and TABS-MD by USACE. REEF3D: SFLOW a 2D numerical modelling is used for the simulation of hydrodynamics and sediment transport for present study.

In the case of 3D models, three-dimensional convection-diffusion and the conservation of mass equation is used to investigate the suspended sediment transport(Van Rijn, 1989). Here the vertical and the horizontal parameters of the sediment transport system is taken into consideration. It requires an extensive amount of data and time consuming for simula-

tion but provides a good quantitative representation of the hydrodynamic structure(Van Rijn, 1989). for e.g. RMA11(Resource management Association, Inc.,2003), DELF-3D, SSIM, and MIKE 3. On using the different numerical models for the simulation of hydrodynamics systems and sediment transport, the final results may have errors or may not provide the actual representations as in the real field. This is due to the errors, uncertainties, and approximation in the algorithms. According to the European Research Community on Flow, Turbulence, and Combustion(ERCOFTAC) have published Guidelines for CFD, in which errors as classified as Olsen (2012):

1. Modelling errors
2. Convergence error
3. Round-off error
4. Numerical approximation error
5. Errors in input data and boundary conditions
6. Bugs in models/software
7. Human errors

3 REEF3D: SFLOW

Time-domain analysis and the representation of the complex free-surface process can be obtained from the phase-resolved wave modeling. For higher resolution near-field wave modeling, it is more important to present the practical wave generation boundary conditions. But far-field wave propagation in the coastal area represents a large-scale phenomenon limiting the implementation of the Navier-Stokes approach. So to model the far-field large-scale phase-resolved wave propagation, the model with less computation requirement should be implemented.

The depth-averaged shallow water model is suitable for coastal wave modeling because coastal areas have shallow water status. For being the two-dimensional model(2D), it requires less cells to present the frequency relation and nonlinearity with the increase of water depth or with varying bathymetry. Boussinesq-type wave model represents shallow water model which provides the information on vertical flow and helps to get the improved frequency dispersion of waves.

Shallow-water models use high-order numerical schemes like fourth-order accurate Adams-Bashforth-Moulton for time discretization, mixed fourth-order and second-order scheme for spatial discretization, and third-order Runge-Kutta scheme for temporal discretization.

REEF3D: SFLOW is composed of hydrostatic and non-hydrostatic shallow water model with the linear and quadratic pressure approximation. The model consists of all existing numerical schemes and parallelization algorithms with a high-order discretization scheme along with the relaxation method for wave generation and absorption. For example, fifth-order weighted essentially nonoscillatory(WENO) scheme in spatial discretization and third- to fourth-order Runge-Kutta scheme is used for temporal discretization.

3.1 Numerical Theory in SFLOW

This section explains the basic principles of the REEF3D: SFLOW model in general along with the formulations and schemes used in the current study.

3.1.1 Mass and Momentum Conservation

The conservation of mass and momentum for an incompressible flow leads to Euler and continuity equations in three dimensions:

$$\frac{\partial U}{\partial x}+\frac{\partial V}{\partial y}+\frac{\partial W}{\partial z}=0 \tag{1}$$

$$\frac{\partial U}{\partial t}+U\frac{\partial U}{\partial x}+V\frac{\partial V}{\partial y}+W\frac{\partial W}{\partial z}=-\frac{\partial P_T}{\rho\partial x} \tag{2}$$

$$\frac{\partial V}{\partial t}+U\frac{\partial U}{\partial x}+V\frac{\partial V}{\partial y}+W\frac{\partial W}{\partial z}=-\frac{\partial P_T}{\rho\partial y} \tag{3}$$

$$\frac{\partial W}{\partial t} + U\frac{\partial U}{\partial x} + V\frac{\partial V}{\partial y} + W\frac{\partial W}{\partial z} = -\frac{\partial P_T}{\rho \partial z} - g \tag{4}$$

where,
U,V,W are velocities in x,y, and z directions
ρ = density
P_T = total pressure and
g= acceleration due to gravity

Here bottom friction and turbulent stresses are excluded but can be included upon required.

3.1.2 Shallow Water Equations

The governing equations considering only depth averaged variable are :

$$\frac{\partial \zeta}{\partial x} + \frac{\partial hu}{\partial x} + \frac{\partial hv}{\partial y} = 0 \tag{5}$$

$$\frac{\partial u}{\partial t} + u\frac{\partial u}{\partial x} + v\frac{\partial u}{\partial y} = -g\frac{\partial \zeta}{\partial x} - \frac{1}{\rho.h}\left[\frac{\partial hq}{\partial x} - 2q\frac{\partial d}{\partial x}\right] \tag{6}$$

$$\frac{\partial v}{\partial t} + u\frac{\partial v}{\partial x} + v\frac{\partial v}{\partial y} = -g\frac{\partial \zeta}{\partial y} - \frac{1}{\rho.h}\left[\frac{\partial hq}{\partial y} - 2q\frac{\partial d}{\partial y}\right] \tag{7}$$

$$\frac{\partial w}{\partial t} + u\frac{\partial w}{\partial x} + v\frac{\partial w}{\partial y} = -\frac{2q}{\rho.h} \tag{8}$$

Equations 6,7 and 8 give the velocity in x,y and z directions respectively.

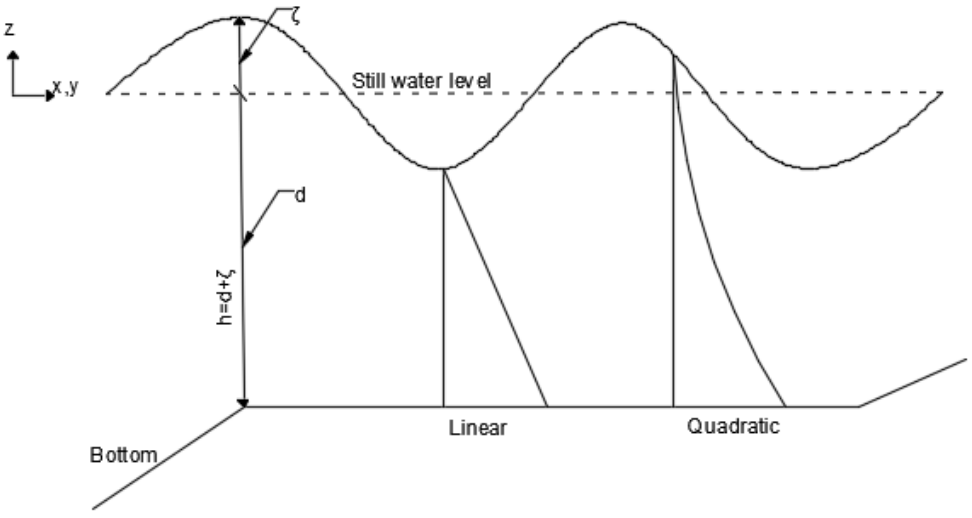

Figure 3: Basic definitions in shallow water model [Redrawn after (Wang et al., 2020) for better readability]

In figure3: h is water depth, d still water depth, and ζ as free surface elevation.
Introducing the quadratic assumption, the governing equations with the depth-averaged variables will be:

$$\frac{\partial \zeta}{\partial x} + \frac{\partial hu}{\partial x} + \frac{\partial hv}{\partial y} = 0 \tag{9}$$

$$\frac{\partial u}{\partial t} + u\frac{\partial u}{\partial x} + v\frac{\partial u}{\partial y} = -g\frac{\partial \zeta}{\partial x} - \frac{1}{\rho.h}\left[\frac{\partial hq}{\partial x} - \left(\frac{3}{2}q + \frac{\rho.h.\phi}{4}\right)\frac{\partial d}{\partial x}\right] \tag{10}$$

$$\frac{\partial v}{\partial t} + u\frac{\partial v}{\partial x} + v\frac{\partial v}{\partial y} = -g\frac{\partial \zeta}{\partial y} - \frac{1}{\rho.h}\left[\frac{\partial hq}{\partial y} - \left(\frac{3}{2}q + \frac{\rho.h.\phi}{4}\right)\frac{\partial d}{\partial y}\right] \tag{11}$$

$$\frac{\partial w}{\partial t} + u\frac{\partial w}{\partial x} + v\frac{\partial w}{\partial y} = -\frac{1}{\rho.h}\left(\frac{3}{2}q + \frac{\rho.h.\phi}{4}\right) \tag{12}$$

The equations are solved on structured staggered grids using FDM. The discretization of convective terms for velocities u,v, and w are solved by using the fifth-order conservative finite difference WENO scheme, (Jiang and Shu, 1996) and third-order Runge-Kutta explicit scheme is used for time discretization(Shu and Osher, 1988).

3.1.3 Dynamic Pressure Solutions

Poissons Equations for dynamic pressure is

$$\frac{h_p}{\rho}\left(\frac{\partial^2 q}{\partial x^2} + \frac{\partial^2 q}{\partial y^2}\right) + \frac{2q}{\rho.h_p} = \frac{1}{\partial x.\partial y}\left(-h_p\left(\frac{\partial u}{\partial x} + \frac{\partial v}{\partial y}\right) - 2w - u\frac{\partial d}{\partial x} - v\frac{\partial d}{\partial x}\right) \tag{13}$$

where,
h_p = water level at the center of the cell.
The parameters like free-surface location ζ, dynamic pressure q, and vertical velocities w are calculated at the center of the cell in a staggered grid, while horizontal velocities are solved at the face of the cell.

To solve the Poisson pressure equation, a high-performance solver library HYPRE is used (Falgout and Yang, 2002). The dynamic pressure q is used to correct the velocities in a correction step.

3.1.4 Wave Generation and Absorption

Dirichlet type of free surface flow is applied as the inlet boundary conditions. When the generation of wave takes place then the free surface is in constant motion and flow direction is varying periodically. So in REEF3D, waves are generated using relaxation method. These

functions are used to generate the wave at the starting and absorb at the end in order to prevent the effects of reflected waves on the wave generation as shown in4.

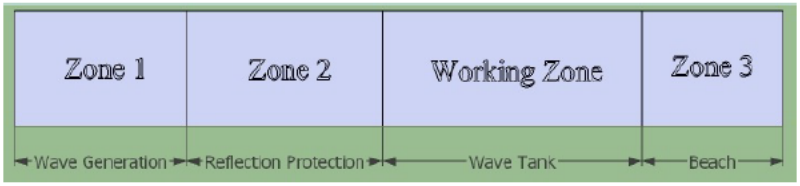

Figure 4: Section of Numberical tank(as in (Kamath, 2012))

Every zone has its own relaxation function. Generation of the wave is taken care by Zone 1, zone 2 prevents the effect of reflected waves and zone 3 absorb the wave which prevents the waves from reflection (Kamath, 2012).

The different parameters like velocities, surface elevations, and pressure are increased to analytical values in Zone 1 and decreased to zero or initial still wave values in Zone 3.

$$u(\bar{x})_{relaxed} = \Gamma(\bar{x})u_{analytical} + (1-\Gamma(\bar{x}))u_{computational} \tag{14}$$

$$v(\bar{x})_{relaxed} = \Gamma(\bar{x})v_{analytical} + (1-\Gamma(\bar{x}))v_{computational} \tag{15}$$

$$\zeta(\bar{x})_{relaxed} = \Gamma(\bar{x})\zeta_{analytical} + (1-\Gamma(\bar{x}))\zeta_{computational} \tag{16}$$

$$p(\bar{x})_{relaxed} = \Gamma(\bar{x})p_{analytical} + (1-\Gamma(\bar{x}))p_{computational} \tag{17}$$

3.1.5 Immersed Boundary

Complex surface geometry exhibits a threat for analysis of flow over bodies with respect to spatial discretization. In the case of a complex flow system, it is not only time-consuming but also difficult to achieve high-quality boundary-equipped mesh creating a problem in the fluid domain while introducing irregular structure(Kajishima and Taira, 2017). Immersed Boundary Method implements the momentum on Eulerian mesh to justify the boundary conditions between the structure and fluid which offers non-body matching the grid structure for complex flow surface(Kim and Choi, 2019). Fig. 6 represents the interpolation of grid using the immersed boundary method.

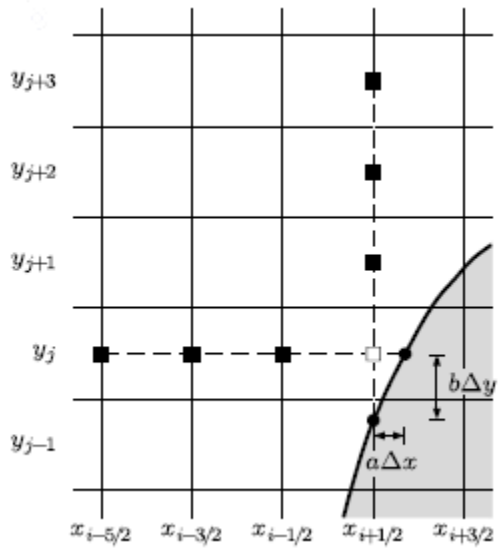

Figure 5: Multi-directional Interpolation (Berthelsen and Faltinsen, 2008)

3.1.6 Parallelization

For any numerical simulation model, it is important to be efficient and effective to solve complex numerical equations for quick results. So to improve the efficiency of the simulation, the software uses multiple processors for computation which is also the same with REEF3D. So under parallel computing, a large problem is broken down into smaller, independent and similar section can be computed simultaneously with the help of multiple processors linking with shared memory(Omnisci, 2021). In REEF3D, the communication is done by ghost cells. Message Passing Interface(MPI) is used to exchange ghost cell value(Afzal, 2013).

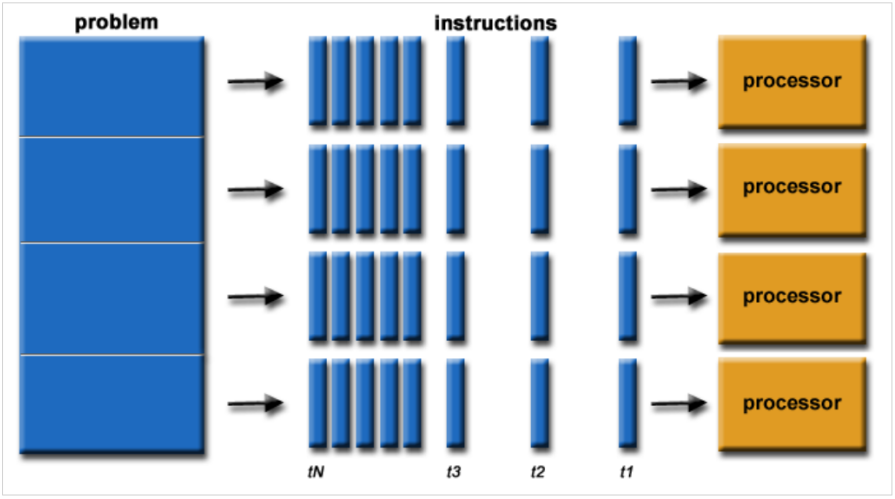

Figure 6: Schematic representation of Parallel Computation (Lawrence, 2021)

3.2 Sediment Transport Modelling

The general practice of sediment transport modeling is to statistical approach in order to evaluate the streamflow pattern and series of sediment discharge as per time and to correspond with the streamflow and sediment discharge data obtained from a lab experiment(Phien and Arbhabhirama, 1979). To quantify the sediment transport, there are different methods which can be applied in any streams or watershed. There are empirical and statistical approaches. Statistical approaches are common in practice as it helps to predict the relationship between the flow discharge and sediment concentration where there is no enough supporting data related to discharge and sediment flow (Aksoy et al., 2019). Sediment transport is a complex process and difficult to quantify the sedimentation process in any watershed, stream, or reservoir. The convenient solution is predicted with the help of a physical or numerical model. But it is difficult modeling the sediment transport modeling because of the effect of scaling laws in suspended sediments and bedload transport(Kobus, 1984). So in order to overcome this problem and get a more reasonable result, the importance of sediment transport modeling is increasing day by day.

3.2.1 Modes of Sediment Transport

Sediment transport occurs when the sediments are carried or eroded by the flowing water, where the motion is controlled by the forces mainly stabilizing and destabilizing(Lysne et al., 2003). The sediment transport process depends upon the settling velocity of sediment and the critical bed stress(Kraft et al., 2011). The sediment is in motion and eroded when the shear stress exceeds the critical shear stress. There are two modes of sediment transport depending on the sediment ratio. They are mentioned below and illustrated in Fig: 7

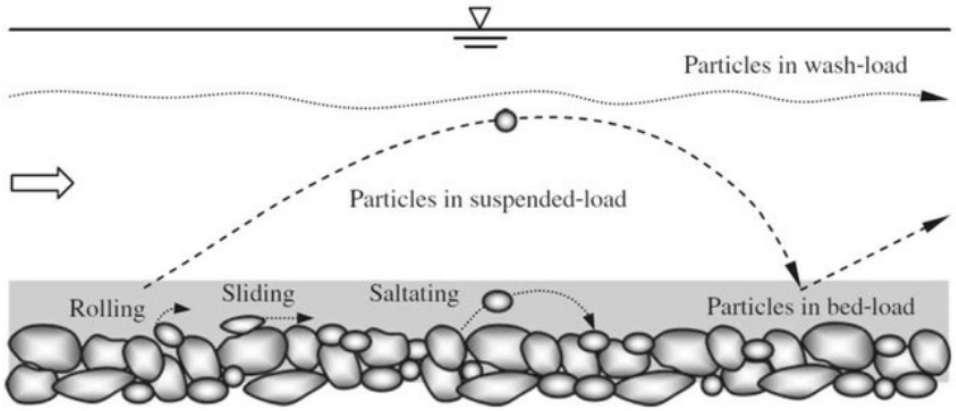

Figure 7: Modes of sediment transport (Dey, 2014)

1. Suspended load
   The suspended load consists of particles, carried by the water flow in suspension. These particles are supposed to move with the almost same velocity as of the flow. Suspended load does not settle on the riverbed but seldom strikes with the riverbed. These loads are expressed in kg/sec and tonnes/day.

2. Bedload
   Bedload includes all the particles which move close to the riverbed. The mode of movement may be sliding, rolling, and saltation and moves much less slower than flow velocity. They come in contact with the riverbed frequently and tend to remain stable.

3.2.2 Bed shear stress

Bed shear stress and shear velocity play a vital role in the mode of sediment transport, deposition, and scour of the channel. It is difficult to measure the boundary shear stress in the complex flow field directly when the flow is three-dimensional(Biron et al., 2004). The bed shear stress can be predicted by relating the boundary shear stress with the velocity of flow conditions(Wilcock, 1996). REEF3D also uses different shear stress formulation conditions which are listed below:

1. Wall Function
   The logarithmic relation between the shear velocity and velocity along the depth is used to calculate the bed shear stress(Wilcock, 1996).

$$\begin{aligned} \frac{u}{u_*} &= \frac{1}{k} ln \frac{z}{z_o} \\ u_* &= \sqrt{\frac{\tau}{\rho}} \\ \tau &= \rho u_*^2 \end{aligned} \tag{18}$$

   Here u is velocity, u_* is shear velocity, z as height above the bed and z_o is the roughness length given by

$$\frac{k_s}{30}$$

   k_s is the bed roughness which depends on grain size. k_s can be estimated using k_s= 3*$d_5$0
   This approach is implemented for sediment transportation in present study.

2. Friction coefficient
In this method, bed friction is used to calculate the bed shear stress.

$$\tau = \frac{\rho f U^2}{2}$$
$$f = \frac{2g}{C^2} \begin{cases} \frac{0.06}{(log\frac{(\frac{12h_s}{3.3\nu})^2}{u*})} & \frac{u*k_s}{\nu} < 5 \\ \frac{0.06}{(log(\frac{12h_s}{k_s})^2} & \frac{u*k_s}{\nu} > 70 \end{cases} \tag{19}$$

3. Velocity based/turbulent viscosity
The turbulent viscosity bed shear stress is given by

$$\tau = -\rho(\nu_t + \nu)\frac{\partial u}{\partial z} \tag{20}$$

ν_t is turbulent viscosity, determined from the turbulence model.

4. Turbulent kinetic based
It correlates the bed shear stress with turbulent kinetic energy. Product of the absolute value of velocity variation from average gives the total kinetic energy.

$$k = \frac{1}{2}\rho(\widetilde{u}^2 + \widetilde{v}^2 + \widetilde{w}^2) \tag{21}$$

$\widetilde{u}$, $\widetilde{v}$, $\widetilde{w}$ are velocity variation in x,y, and z directions. The relation between shear stress and kinetic energy is given as

$$\frac{\tau}{k} = \sqrt{c_\mu} \tag{22}$$

3.2.3 Bed Load Transport

Different formulas are developed to calculate the bed-load transport. Lots of empirical observations are integrated with the theory and a suitable formula is proposed based on the observed value and applicable for similar site conditions(Lysne et al., 2003). Bedload transport formula correlates transport rate with the shear stress.

$$\begin{aligned} \tau* &= \frac{\tau}{(\rho_s - \rho)gd} \\ \tau_c* &= \frac{\tau_c}{(\rho_s - \rho)gd} \\ q_b* &= \frac{q_b}{\sqrt{\frac{(\rho_s - \rho)g}{\rho}}d} \end{aligned} \tag{23}$$

ρ_s denotes the density of sediment,ρ density of water, d as sediment particle diameter, and g denotes gravity. q_b* represents bedload transport and $\tau*_c$ denotes critical shear stress and $\tau*$ as shear stress which are dimensionless parameters.
REEF3D uses different bedload transport formula which are listed below:

1. Meyer-Peter and Muller
   It was one of the oldest and widely used equations developed by Meyer-Peter and Muller. The proposed formula was:

$$q_b* = \alpha_s(\tau* - \tau_c*)^{\frac{3}{2}} \tag{24}$$

   τ_c* is dimensionless critical stress equal to 0.047.The value of α_s is 8(Wiberg and Dungan Smith, 1989).
   Bedload transport depends on the bed shear stress. If the shear stress exceeds 0.047, the transport of bedload initiates. Critical shear stress is calculated using the shield diagram.

2. Van Rijn
   The bedload transport formula given by Van Rijn is

$$0.053\frac{(\frac{\tau-\tau_c}{\tau_c})^{2.1}}{(d_i\frac{(\frac{\rho_{sg}}{\rho-1})^{\frac{1}{3}}}{v^2})^{0.3}} \tag{25}$$

   v is the kinematic viscosity of water. τ_c critical shear stress and d_i is sediment particle diameter.

   Van Rijn approach is used to calculate the bedload transport in present study.

3. Engelund and Fredøse
   The relation for the bed load transport is give as

$$q_b* = 18.74(\tau* - \tau_c*)(\tau*^{0.5} - 0.7\tau_c*^{0.5}) \tag{26}$$

   This relation is applicable for fine to medium sandOdnature (2021)
   .

3.2.4 Bed Morphology: Model-Level Set Method

Osher and Sethian proposed the level set method in order to route movable sediment surfaces(Osher and Sethian, 1988). It depends on the two central propositions .i.e. embedding the interface to zero level set of function with higher dimension and extension of interface velocity to function with higher dimension level set(Kraft et al., 2011).
The evolving interface is denoted by function ϕ=0. The equation for the evolution of ϕ correlating to the motion of interface is

$$\frac{\partial\phi}{\partial t} = F|\nabla\phi| = 0 \tag{27}$$

where F is propagating velocity of the interface along its normal direction and given by:

$$F = \frac{\partial z_b}{\partial t} \tag{28}$$

z_b is the local bed surface elevation.
It tracks all the level sets over the whole domain, even though interest is confined only to zero level set. This level-set Method is applied in REEF3D to track moveable sediment surfaces.

3.2.5 Bed Shear Stress Reduction

With a constant, the critical condition for sediment transport helps to determine the rate of bedload transport. The threshold for the sediment transport can be obtained from Shield's diagram which only accounts the forces for equilibrium conditions but not the bed slope (Afzal et al., 2020). For correct shear stress, additional gravitational and tractive components should be included along with the hydrodynamics forces. The critical shear stress τ_o from a flat bed is multiplied by the reduction factor r.

$$\tau_c = r * \tau_o \tag{29}$$

3.2.6 Sandslide

Initiation of bed erosion causes tiltation of bed cells which reduces the critical shear stress on the respective cells. This results in further erosion making the bed slope more steeper with continuous erosion. So application of sandslide algorithm is required to limit the reduction of bed shear stress. After being the bed slope greater than the angle of repose, The slope of a cell is readjusted distributing the volume of sediment to its neighboring cell until the bed slope is equal to the angle of repose. In the current study, sand slide algorithm is implemented to limit the never-ending erosion process.

4 Project Description

4.1 Background

Binga Hydroelectric Power Plant is a storage type reservoir with an installed capacity of 100 MW later upgraded to 140 MW, located in Benguet province of Philippines. It is located 19 km downstream from Ambuklao hydropower and Adonot River and Bisal River are its major tributaries. The type of dam is Earth and Rockfill with 215 lengths and a height of 107.37 m. Power Intake is located at the right side of the dam whereas spillway to the left abutment. The crest level of the dam is 586 masl with the maximum and minimum operating level of 575 and 566 masl respectively. The intake invert level is 555 masl. The project utilizes the net head of 156 m and design discharge of 25 m^3/sec and generates 238.43 GWh annually from 4 vertical Francis turbine of 35 MW each (iha, 2021).

Figure 8: Binga Hydropower plant(Obtained from Google Earth)

After the completion of a project, sediment gets rapidly filled in the reservoir area due to the lack of the flushing facilities like bottom outlet. Since the heavy sediment flows from its tributaries, a sediment delta is formed in the reservoir approaching the dam. The sedimentation shorten reservoir lifetime along with the damages on hydropower components.

Therefore, the physical model experiment was planned and carried out at Norsk Hydroteknisk Laboratorium, Norwegian University of Science and Technology (NTNU) to study the sediment transport mechanism under the different discharge conditions along with the test of the efficiency of the Sediment Bypass Tunnel. The physical model has been set up with a scale of 1: 66.67 using Froude law for scaling. The general layout of the physical model is shown in Fig: 9. The model is facilitated with the sediment feeder, and four control points (denoted by CP) at different locations to observe the water elevation during the flushing period.

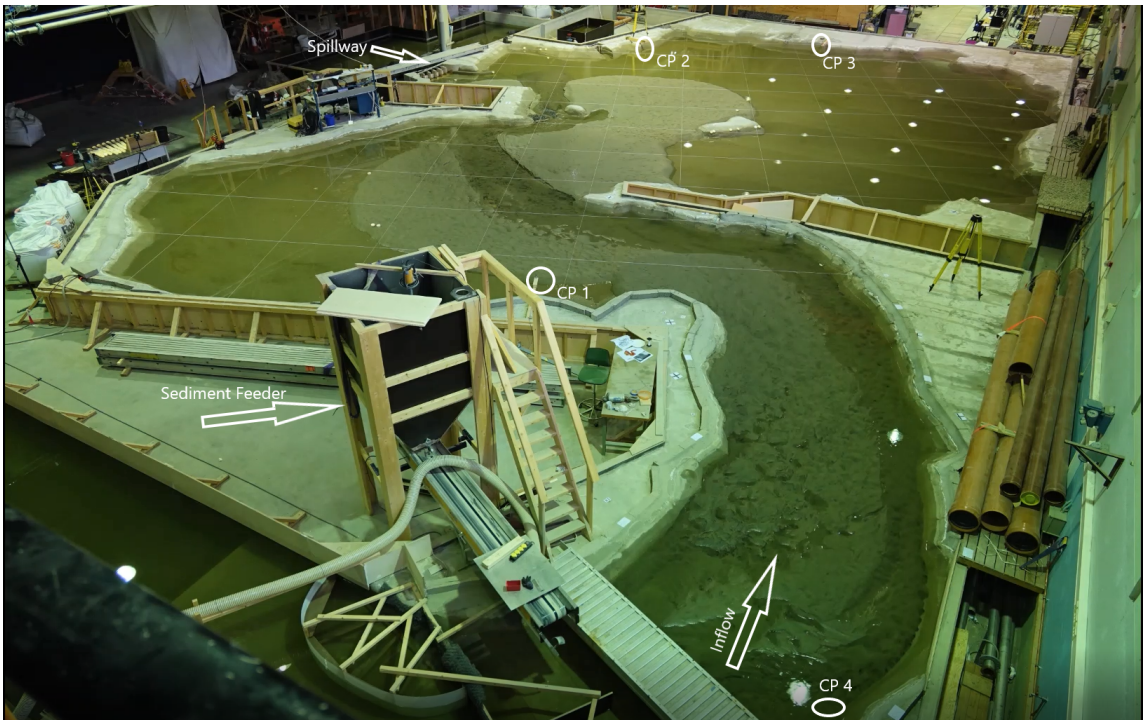

Figure 9: Layout of Physical Model (adopted from lab)

4.2 Results from Physical Model

The drawdown flushing was carried out with two different constant inflow discharges of 500 m^3/s and 1000 m^3/s. The pattern of erosion and deposition of sediment was observed and compared with the initial bed level. The area inside the rectangular box as in Fig: 10 represents the area of interest for sediment deposition and erosion. The initial bed and bed after flushing with 500 m^3/s and 1000 m^3/s are shown in Fig: 10.

After flushing with 500 m^3/sec significant bed changes were observed in the Area II and III whereas no considerable changes were witnessed at Area I as shown in Fig: 10 (b). In area II erosion of bed by 4 to 7 can be observed which results the formation of channel as illustrated in Fig: 10(b). Some of these eroded material are deposited at the left bank of downstream bend in area II and reaming portion are transferred to further downstream. The bed is increased by 6 to 9 cm in Area II. Similarly, in Area III a delta of sediment can be observed approaching toward the spillway section with bed rise of 12 to 15 cm. The rise and fall in bed level after flushing is represented in Fig: 11(a). The overall view of deposition and erosion pattern in different section is shown in Fig: 12(a).

Fig: 10(c) shows the changes in bed level after flushing with 1000 m^3/sec. The erosion of sediment took place at the inlet section which then deposited in the right bank increasing the bed level by approximately 3 cm. However the bend section at downstream of Area I remains unchanged. The channel formed after flushing with 500 m^3/sec in Area II is further scoured resulting the wider and deeper section. The depth of channel is increased by 3 cm. The sediment delta is further shifted towards the spillway section and finally downstream of spillway. The change in bed level and the area of scouring and deposition is further represented in Fig: 11(b) and Fig: 12(b)

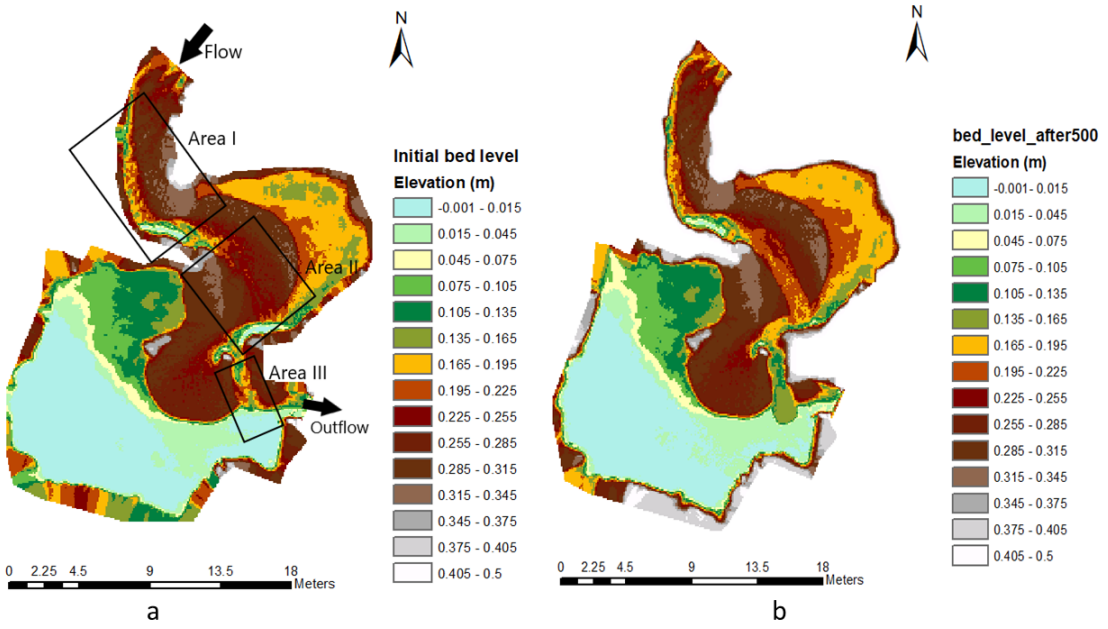

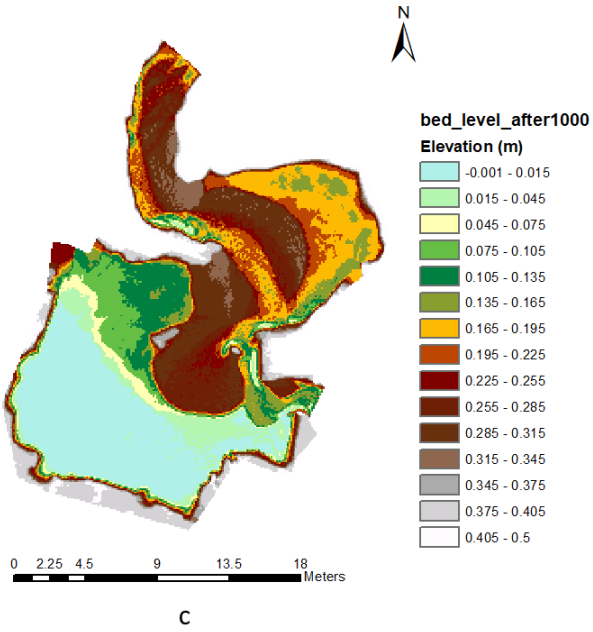

Figure 10: Measured initial bed level(a), bed level after flushing with 500 m^3/sec(b) and bed level after flushing with 1000 m/sec(c)

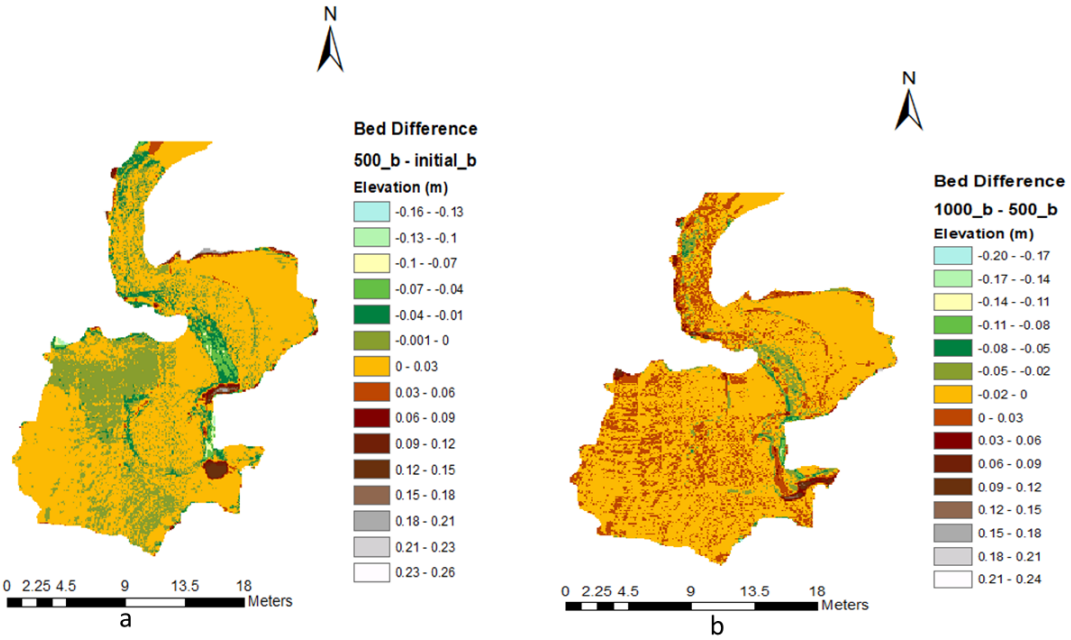

Figure 11: Difference on bed level after flushing: bed level difference after flushing with 500 m^3/sec(a) and bed level difference after flushing with 1000 m/sec(b)

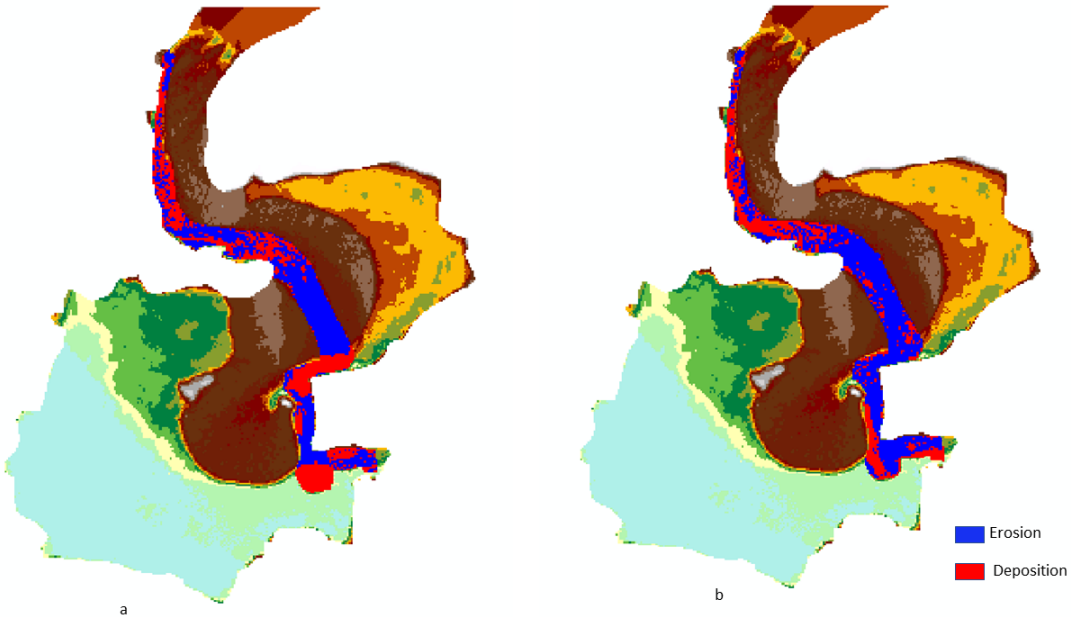

Figure 12: Change in sediment volume after flushing with 500 m^3/sec(a) and 1000 $m^/sec$(b)

After scouring and deposition, the change in bed level occurs which can be represented in terms of cut and fill volume. To get the overview on change in volume in bed level, the bathymetry is used to calculate the net deposition and loss in volume after flushing with 500 and 1000 m^3/sec using Arc gis as shown in Fig: 12. The obtained net deposition and erosion after flushing with 500 m^3/sec was 0.6008 m^3 and 0.509 m^3 respectively. While flushing with 1000 m^3/sec scoured volume was 0.453 m^3 and deposition was 0.213 m^3.

5 Hydrodynamic Simulation

Hydrodynamic simulation is the process with which the flow is simulated including the interactions with the structure/obstacles. It is very important to have a stable hydrodynamic simulation before compiling the sediment simulation. It measures the degree of accuracy of the model in representing the real-world concept(Committee, 1998). This method helps to decide the appropriate grid size, wall roughness, discharge, and discretization scheme, which can be implemented in sediment simulation.

5.1 Numerical Model Validation

To calibrate and validate any numerical model, at least two sets of data are required. In order to calibrate and validate the REEF3D: SFLOW model, data were collected from the lab experiment, and a computational mesh/model was created. The model was calibrated with bed bathymetry, water surface elevation, and outflow discharge at the spillway and the inflow discharge. After then, the model was validated with the measured water surface elevations at different control points and velocity inflow profile.

5.1.1 Data Collection and Interpretation

Water surface elevations, bed bathymetry, and the velocity profile were obtained from the different sections of the physical model in the lab with the flow conditions of 0.0286 m^3/sec(1000 m^3/sec in prototype model), which are used for the model calibration and validation. Water Surface elevations were measured at three different locations (control points) with the help of sensors. Inflow velocity data were collected just downstream of the inflow section at a different distance from the left bank of the model.

5.1.2 Simulation Condition and Input Parameters

For hydraulic simulation, a steady-state computation is provided with the fixed water surface and fixed bed. The water level surface is fixed at 0.305 masl (575.33 masl in prototype) using the F 60 command in the control file. The inflow discharge of 0.0286 m^3/sec (1000 m^3/sec in prototype) is provided at the upstream end, and outflow of the same discharge is maintained at the spillway gates considering the rating curve of the spillway with the command B 412 in the control file. The topography data set is provided with the geo.dat file, and grid size of 5 cm is constructed using the B 10 command. The topography is rotated at 29 degree about a fixed point to align the intake and outlet location with the domain side.

5.1.3 Calibration and Validation Results

The calibration and validation technique includes the comparison of the water surface elevations at three locations and one cross-sectional velocity profile with those measured in the physical model. For adjustment of the model with the measured water surface elevations and velocity profile, different Manning's roughness coefficient(n) ranging from 0.0142 to

0.02 was assigned to know the best-fitted model conditions. The accuracy of the models' predictions with respect to Manning's value were analyzed using different statistical methods, including mean absolute relative error (MARE), mean absolute error (MAE), root mean square error (RMSE), and linear correlation coefficient between physical (O_i) and simulated model(P_i) values using Eqs(30-32)

$$RMSE = \sqrt{\frac{1}{n}\sum_{i=1}^{i=n}(O_i - P_i)^2} \tag{30}$$

$$MAE = \frac{1}{n}\sum_{i=1}^{i=n}|O_i - P_i| \tag{31}$$

$$MARE = \frac{100}{n}\sum_{i=1}^{i=n}\left|\frac{O_i - P_i}{P_i}\right| \tag{32}$$

In Table 1, the water elevation values of the physical and simulated model are presented. These values were then used to perform the statistical analysis, and results were listed in the Table 2. The statistical indices thus computed were compared to find the best-fitted model condition. The results from RMSE, MAE, MARE show the decreasing trend of error values with increasing Manning's value which does not show conclusive result. At the same time, R square values increase with increase in Manning's value and achieve peak value at Manning's value 0.0166 and again decrease with further increase in Manning's number.

Table 1: Simulated Model Water Surface Elevation with different Manning's Values

Control Point	**Physical Model**	**Water elevation at different Manning's Value(m)**					
		0.02	**0.0181**	**0.0166**	**0.0142**	**0.0125**	**0.0111**
1	0.3052	0.3060	0.3059	0.3057	0.3058	0.3059	0.3057
2	0.3014	0.3061	0.3061	0.3061	0.3061	0.3060	0.3060
3	0.3005	0.3065	0.3065	0.3062	0.3064	0.3064	0.3063

Table 2: Comparing the performance of model using statistical indices

Manning's Value	**Stastical Index**			
	RMSE	**MAE**	**MARE**	**R Square**
0.02	0.0044	0.0038	1.2549	0.6316
0.0181	0.0043	0.0037	1.2375	0.7536
0.0166	0.0043	0.0037	1.2182	0.974
0.0142	0.0043	0.0036	1.2047	0.881
0.0125	0.0042	0.0036	1.1826	0.736
0.0111	0.0042	0.0036	1.1809	0.863

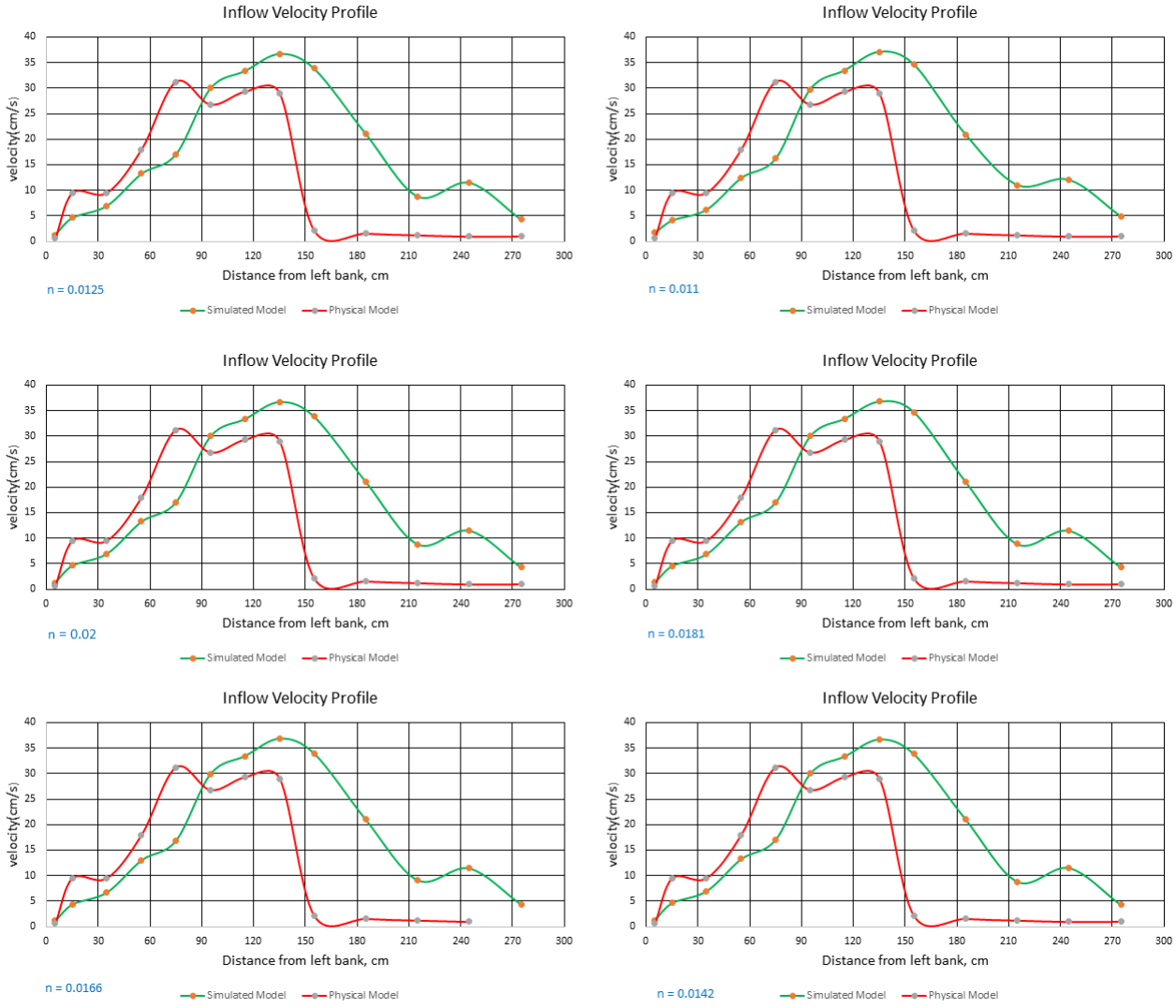

Figure 13: Physical and Simulated model- inflow velocity profile

The simulated velocity magnitude and distributions are compared well with the physical model. Comparison of physical and simulated model-velocity profile for the given cross-section with different Manning's values is shown in Fig: 13. The shape of physical and simulated model-velocity distribution were similar. At the cross-section in the physical model where the velocity measurement was carried out, the average velocity was found to be 12.366 cm/sec. The averaged simulated velocity from the numerical model are shown in Table 3. In a comparison of measured averaged velocity with simulated velocity, Manning's value 0.0166 gives the closest average velocity which is 17.108 m/sec From statistical analysis and velocity profile comparison, Manning's value 0.0166 gives the best fitted model condition. This value of Manning's coefficient is then used for further numerical analysis of sediment flushing.

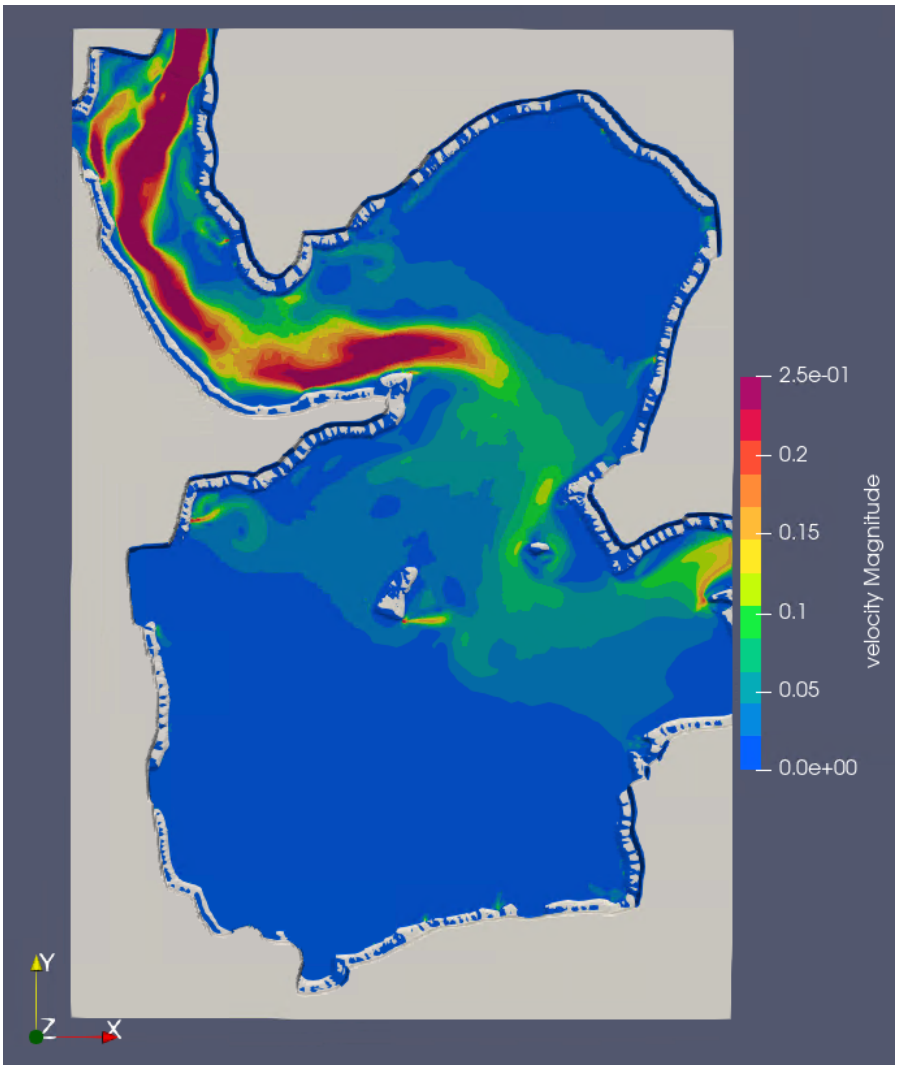

Figure 14: Flow velocity Pattern in Simulated Model

Table 3: Averaged simulated velocity with different Manning's Value

Manning's Value	Averaged Simulated Velocity
0.02	17.148
0.0181	17.194
0.0166	17.108
0.0142	17.246
0.0125	17.275
0.0111	17.253

6 Sediment Flushing

On the basis of the result from the hydrodynamic simulation, the global roughness coefficient (Manning's value) of 0.0166 and the grid size of 5 cm was implemented to carry out the sediment simulation in REEF3D: SFLOW. The grid for the computation of flushing of 500 m^3/s and 1000 m^3/s was constructed using the bathymetric data obtained from the Norsk Hydroteknisk Laboratorium, Norwegian University of Science and Technology (NTNU). The hydrograph of inflow water level, outflow water level, and the outflow discharge were used as the boundary conditions in both cases as shown in Fig:15 and Fig: 16 . The density of bed material was supposed to be 2650 kg/m^3. Along with this uniform bed material of size d_{50} 0.027 m (obtained from NTNU lab) was applied for simulation. For validation of both models, simulated and physical modeled drawdown water elevations were compared at different time intervals. In addition, final simulated bed topography was compared with the actual bed , both quantitatively and qualitatively.

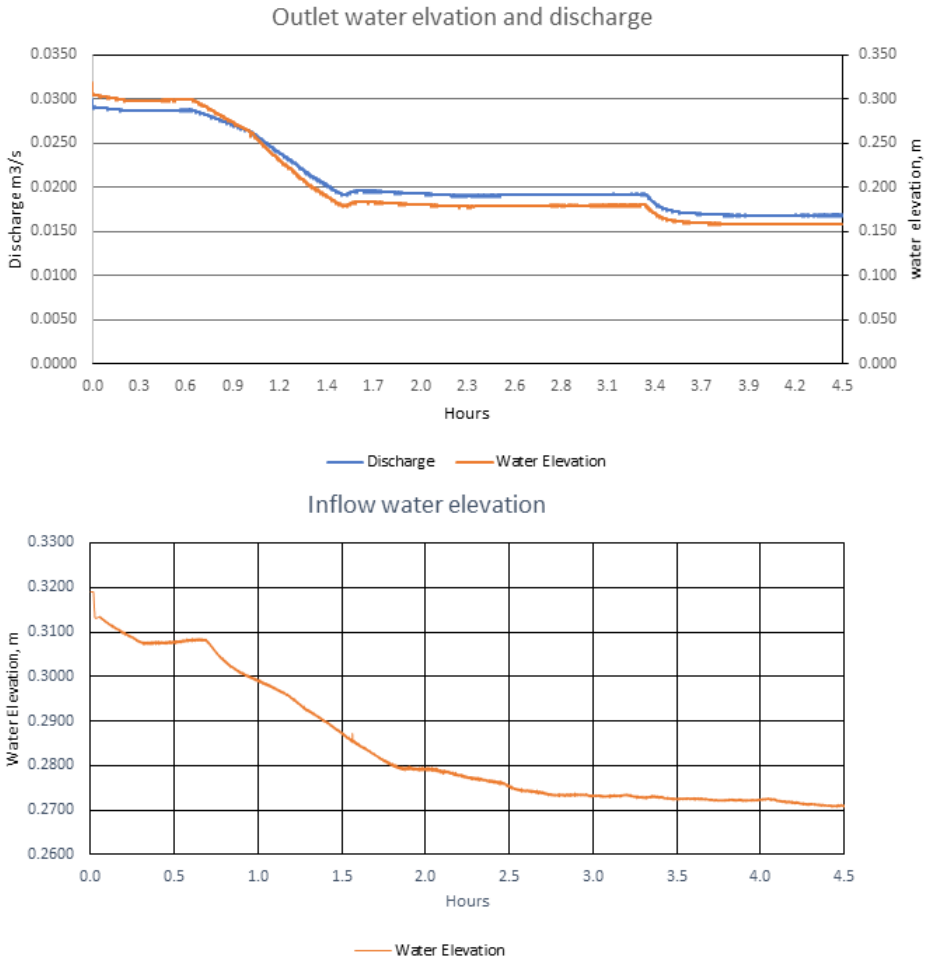

Figure 15: Measured inflow water elevation and outflow discharge and water elevation for 500 m^3/sec

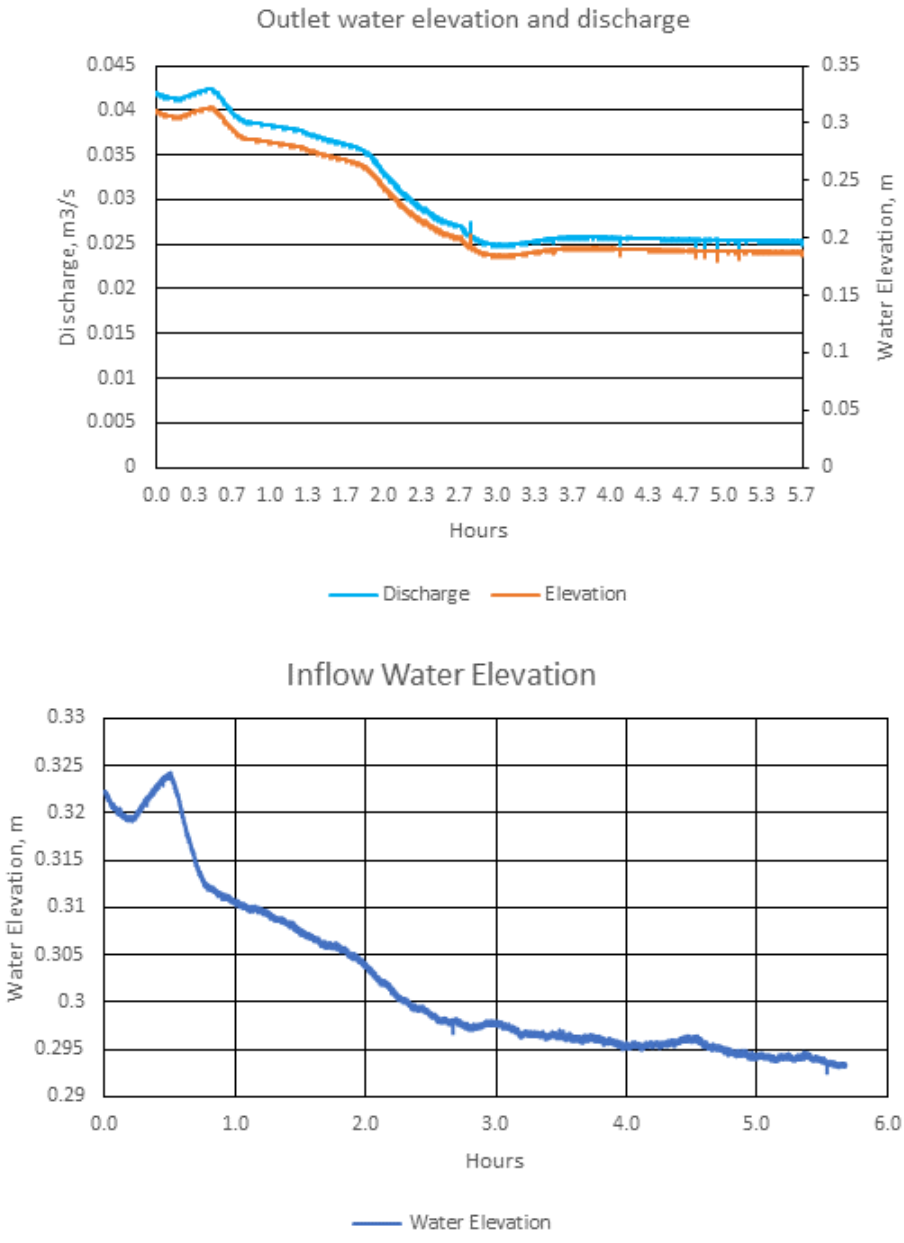

Figure 16: Measured inflow water elevation and outflow discharge and water elevation for 1000 m^3/sec

6.1 Flushing Procedure

Flushing operation was done by drawing down the reservoir water level through the spillway gates. There was no inflow into the power intake. The drawdown flushing was carried out with two discharges i.e. 500 m^3/sec and 1000 m^3/sec. Initially, discharge of 500 m^3/sec was used for flushing and then 1000 m^3/sec.

6.1.1 Flushing with 500 m^3/sec

At the beginning of the experiment, the reservoir level was maintained at 0.307 m (575.5 masl in prototype) with the constant inflow of 500 m^3/sec. In order to pass the discharge, the spillway gates were opened slowly limiting the flow of 1000 m^3/sec following the rating curve of spillway. The draw down process was done in three steps. At the first step, the water level was dropped to 0.178 m (567 masl in prototype) and after achieving this level, the model was run for one and half hours. Then slowly spillway gates were further opened to have free flow condition at spillway. The recorded water elevation was 0.158 m (565.6 masl in prototype) at power intake during free-flow condition. The water level drawdown with spillway discharge is shown in Fig: 15.

6.1.2 Flushing with 1000 m^3/sec

At the start of the experiment, the reservoir level was maintained at 0.310 m (575.7 masl in prototype) with the constant inflow of 1000 m^3/sec. Then spillway gates were opened slowly to pass the discharge limiting the flow of 1500 m^3/sec following the rating curve of spillway. The draw down process was done in two steps. At the first step, the water level was dropped to 0.188 m (567.6 masl in prototype) to achieve the free flow condition. This step lasts for two and half hours. And after achieving free flow condition at spillway the model was ran for three more hours. The water level drawdown with spillway discharge is shown in Fig: 15.

6.2 Simulation of Flow Field and Morphological Bed Changes

6.2.1 Flushing with 500 m^3/sec

Drawdown flushing operation was initiated by opening the spillway gates as per the spillway rating curve until reservoir water elevation reached to 0.178 m. Fig: 18 illustrates the bathymetry arrangement along with the surface velocity field at the beginning of drawdown(a), intermediate drawdown stage(b), and freeflow condition(c) with the lower water elevation of 0.158 m. The grids were not included on the computation which are associated with the lower water level than the assigned wetting/drying condition. The implementation of the wetting/drying algorithm helps to adjust grid and eventually the flow achieves the specific direction as shown in Fig: 18(a,b,c). At the initial stage of drawdown, the velocity was higher at the upstream of Area I which later shifted to downstream of Area II contributing to initiation of erosion and deposition process on the respective areas as shown in Fig: 19(a). Later the erosion extended toward the upstream of Area II followed by deposition at downstream. Like Area II, similar pattern can be seen as in Area III as illustrated in 19(b). After achieving the free flow condition, the velocity increases up to 0.44 m/sec at the bend of Area III, which forms the erosion channel at upstream of Area III, resulting in sediment hump at downstream. At this condition, an increase in bed level due to deposition can be observed near the bend. The final change in bed level ranges from -2 to -7 cm, and 2 to 15 cm was recorded at the upstream and downstream section of Area II respectively. And

in case of Area III, bed gets eroded by 2 to 12 cm at upstream and bed level increases by 13 cm by sediment deposition at downstream of Area III approaching the spillway section as illustrated in Fig: 20 whereas no considerable changes in bed level were seen in Area I. Comparing the water elevation during flushing at Control point 1 and 3 with the physical mode, both control points follows the similar pattern as in Physical model. The comparison of water surface elevation is shown in Fig: 17

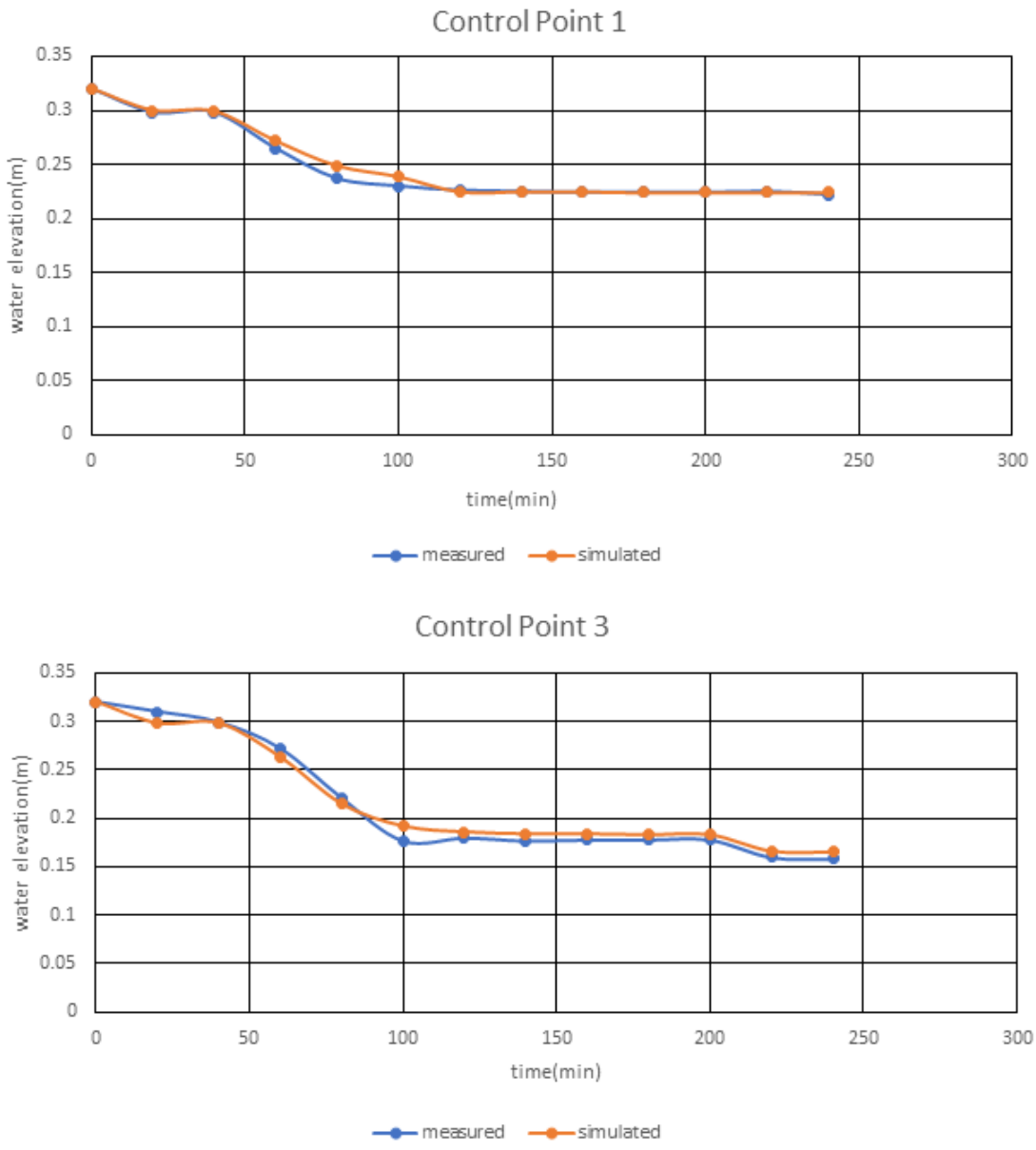

Figure 17: Simulated and Physical Model Water elevation comparison at Control Point 1 and 3

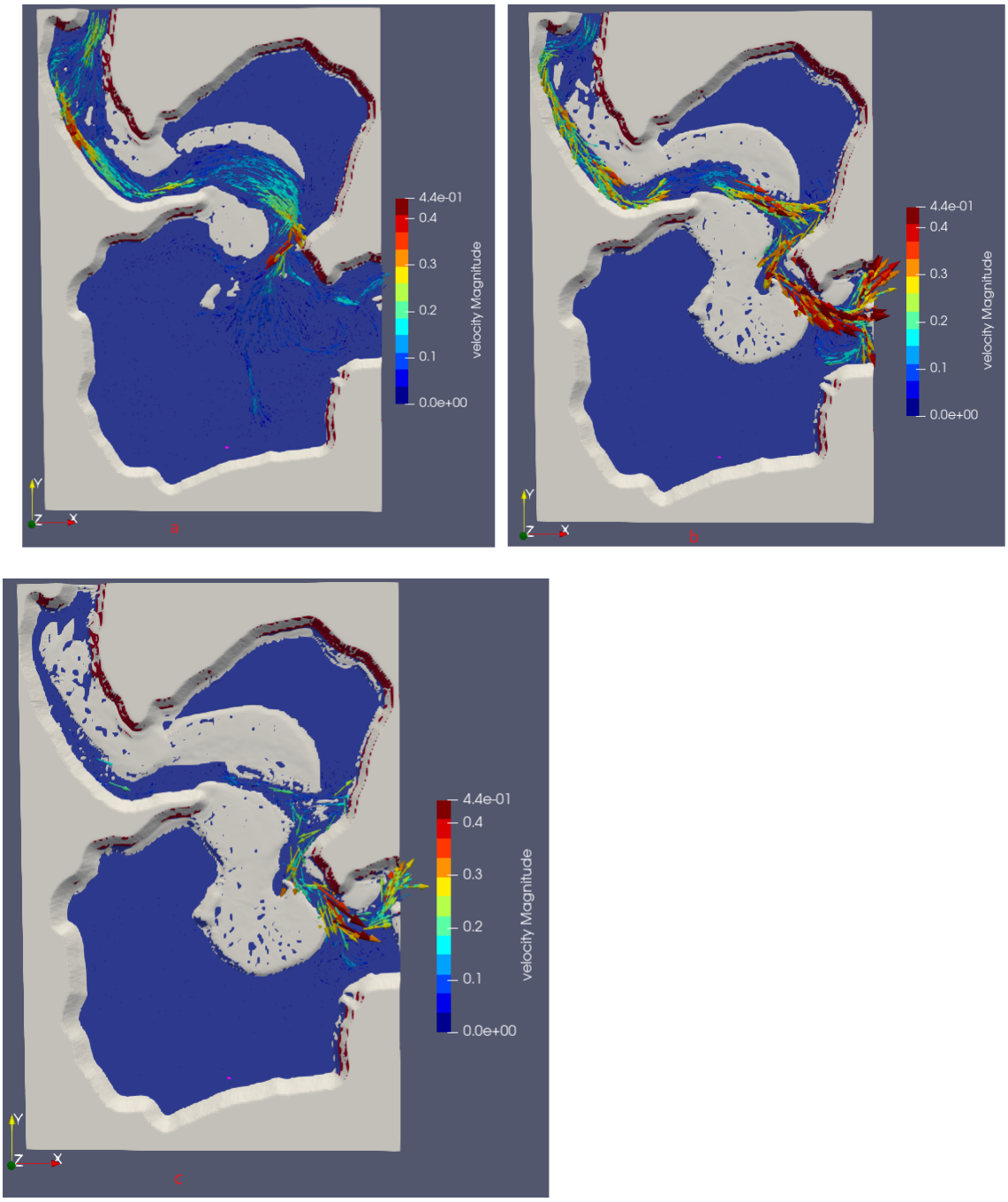

Figure 18: Computational bathymetry and corresponding surface velocity (a) at initial stage of drawdown, (b) intermediate drawdown stage(t= 1.5 h) and (c) during free-flow condition(t= 3 h)

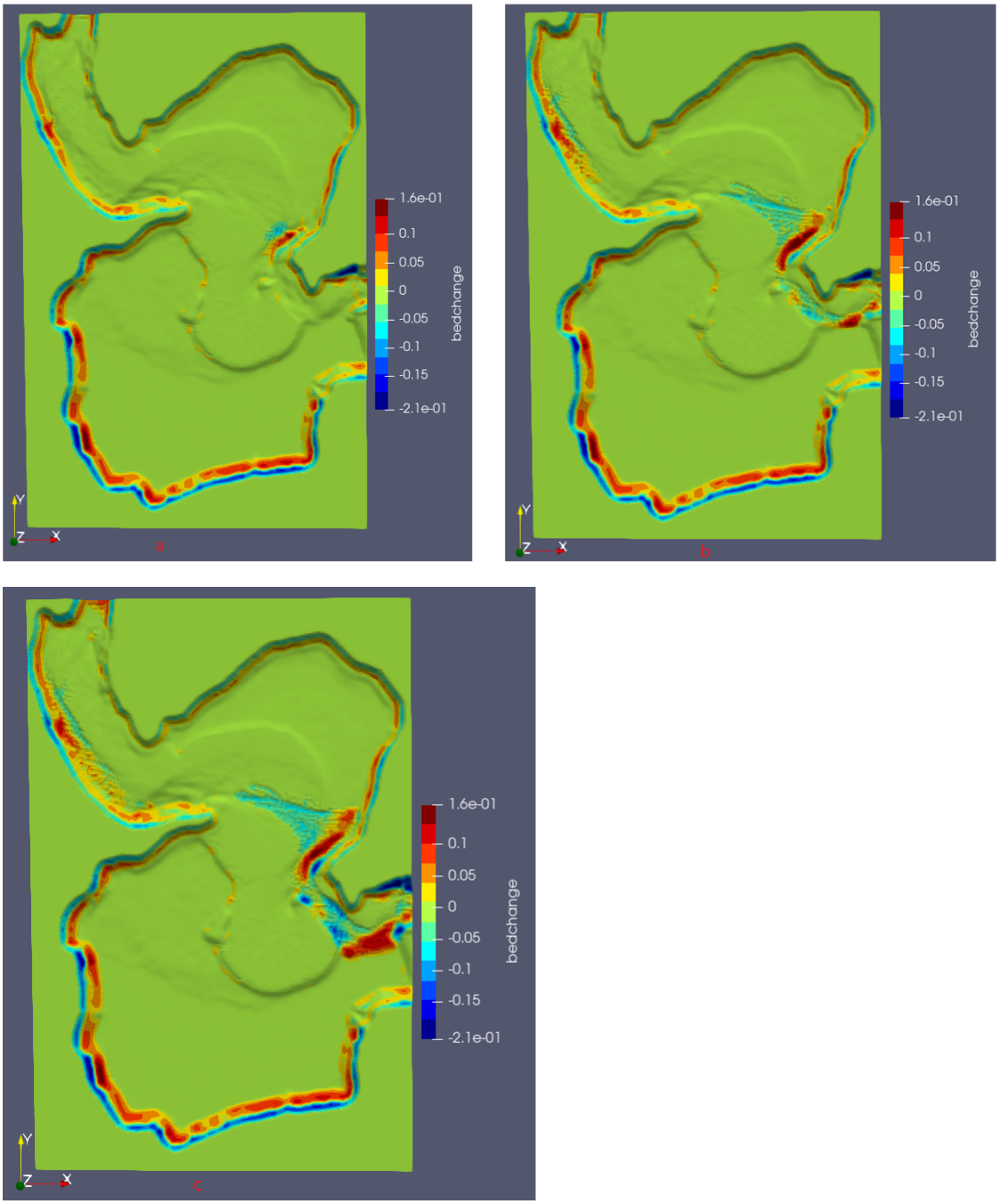

Figure 19: Morphological bed change (a) at initial stage of drawdown, (b) intermediate drawdown stage(t= 1.5 h) and (c) during free-flow condition(t= 3 h)

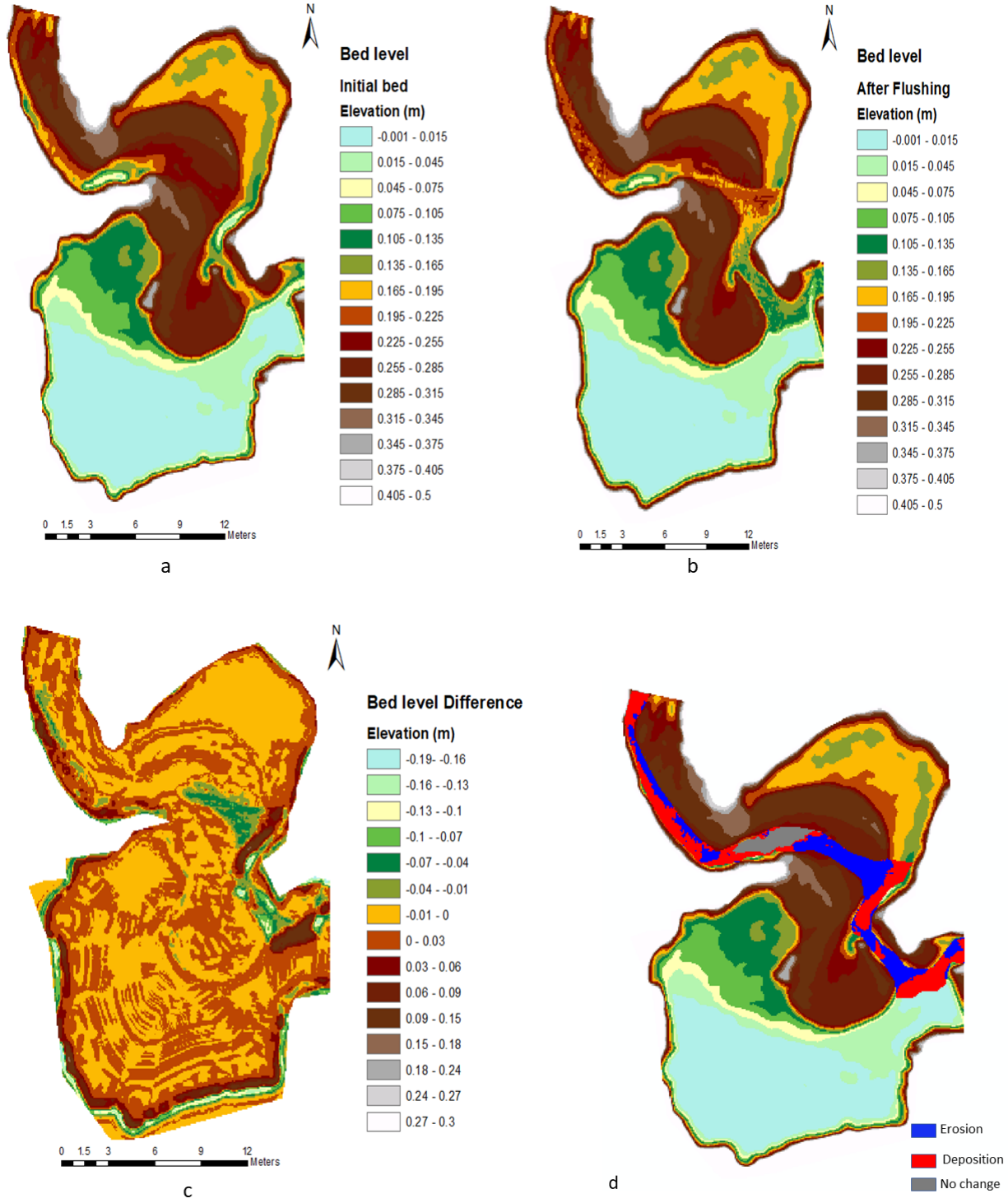

Figure 20: Simulated initial bed level (a), bed level after flushing (b), and bed level difference (c) change in sediment volume (d) (extracted from Arcgis)

In order to compare the result of change in volume of bed level obtained from physical model, net gain and loss in volume after flushing with 500 m^3/sec was calculated from the simulated topographic data. The net gain in volume was found to be 0.656 m^3 and loss as 0.482 m^3.

6.2.2 Flushing with 1000 m^3/sec

After completion of flushing with 500 m^3/sec, constant discharge 1000 m^3/sec was allowed to flow over the same bed maintaining the reservoir level at 575.7 masl. Spillway gates were slowly opened to initiate the flushing operation. As soon as reservoir drawdown took place, the velocity reaches up to 0.41 m/sec commencing erosion and deposition of sediment in Area I which further keeps on developing towards the inflow section as shown in Fig: 22 (a) and (b). The sediment got deposited at the bend downstream of Area I by approximately 4 to 15 cm. After some time supercritical flow will occur achieving the free flow condition which results in high velocity at Area III. This kind of flow condition contributes on more erosion of bed transporting the sediment towards the spillway section as presented in Fig: 23 (c). From Fig: 23, 3 to 15 cm of sediment delta formed near the spillway section. Regarding Area II, the scouring and deposition is up to 7 and 5 cm respectively resulting a scoring channel. Comparing the water elevation during flushing at Control point 1 and 3 with the physical mode, control points 3 well resemblances with physical model whereas water elevation for control point 1 decreases by a maximum 1 cm after 3 hrs which is shown in Fig: 24.

Change in volume of bed level obtained from physical model is compared with net gain and loss in volume after flushing with 1000 m^3/sec was calculated from the simulated topographic data. The net deposition after simulation was found be 0.7233 m^3 and erosion as 0.0.587m^3.

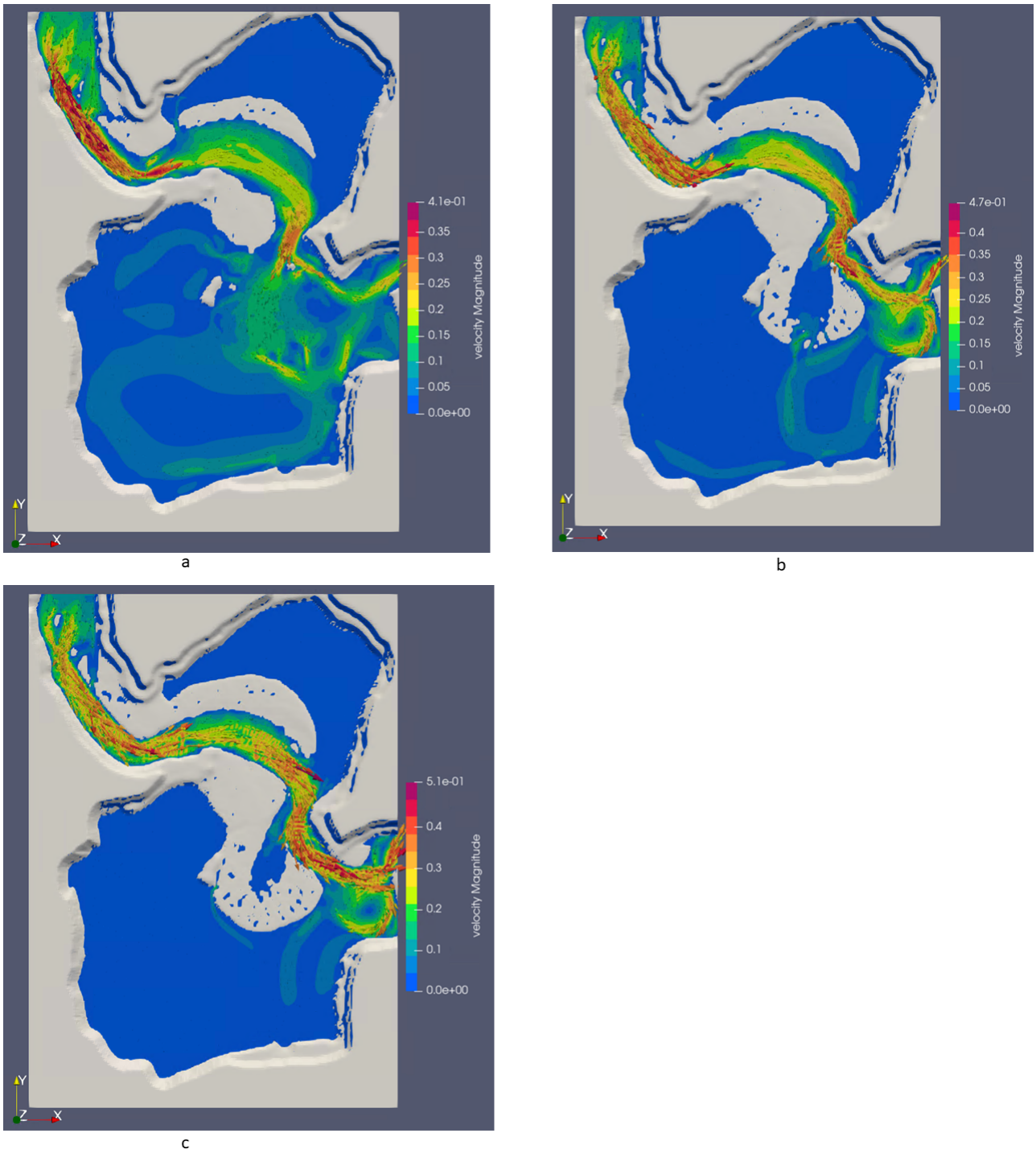

Figure 21: Computational bathymetry and corresponding surface velocity (a) at initial stage of drawdown, (b) intermediate drawdown stage(t= 2 h) and (c) during free-flow condition(t= 3 h) (extracted from REEF3D:SFLOW)

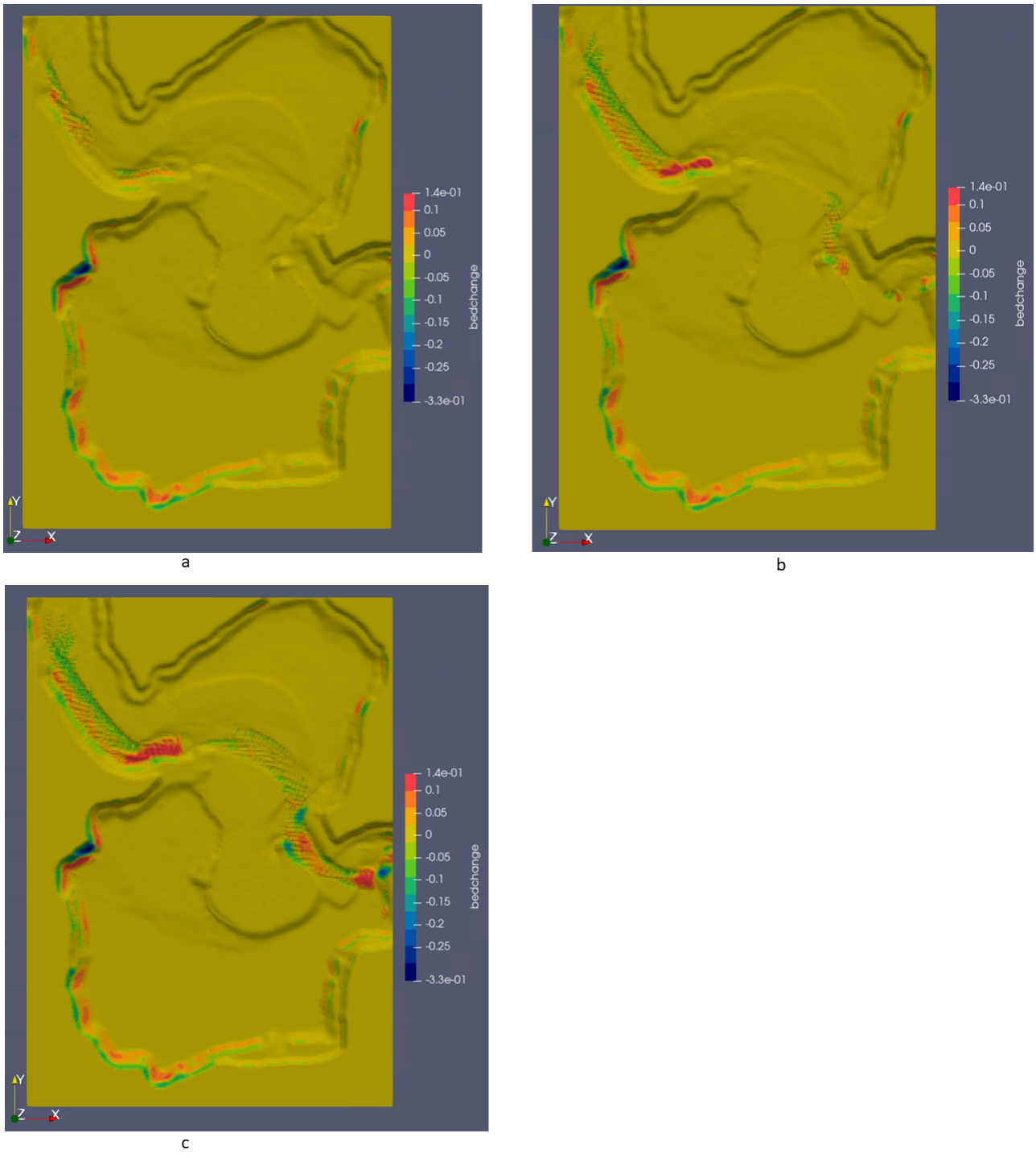

Figure 22: Morphological bed change (a) at initial stage of drawdown, (b) intermediate drawdown stage(t= 2 h) and (c) during free-flow condition(t= 3 h) (extracted from REEF3D:SFLOW)

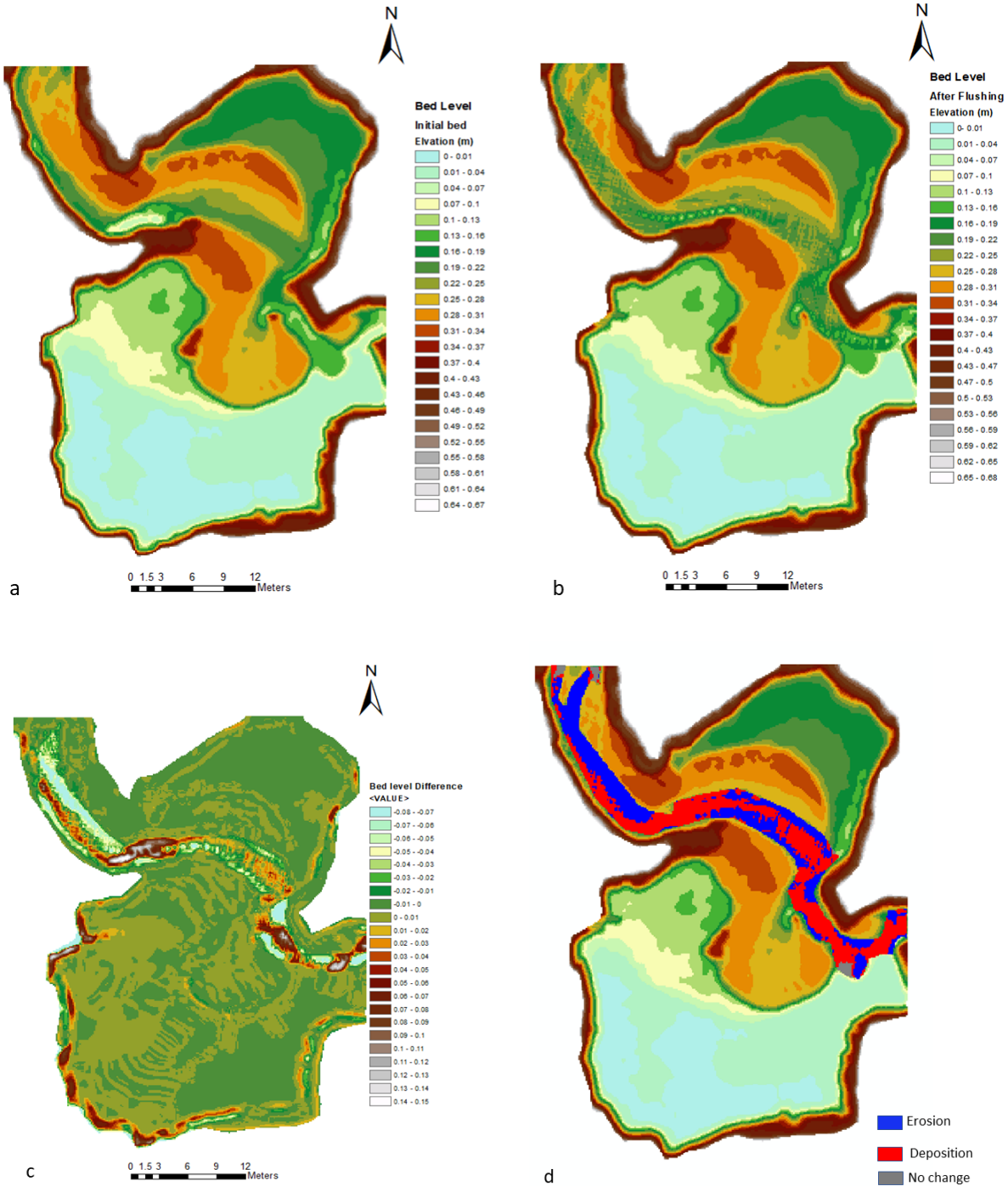

Figure 23: Simulated initial bed level (a), bed level after flushing (b), bed level difference (c) and change in sediment volume (d) (extracted from ArcGis)

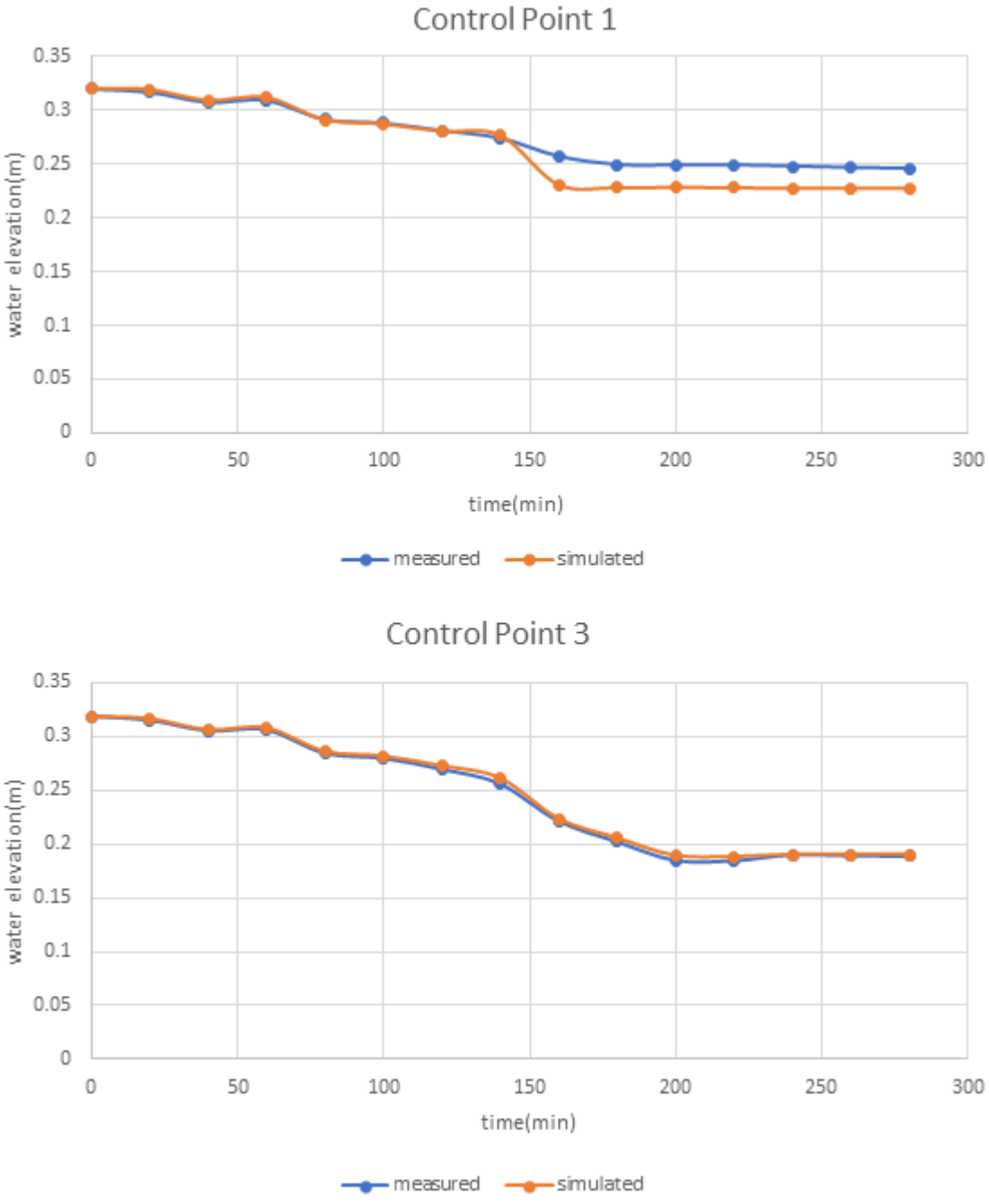

Figure 24: Simulated and Physical Model Water elevation comparison at Control Point 1 and 3

7 Discussion

From the hydraulic simulation,flow pattern and distribution show fair comparison to the physical model whereas variation in velocity magnitude and surface water elevation at different control points were observed. Fig: 14 represent simulated flow pattern and Fig: 13 shows velocity magnitude difference. The water surface elevation is illustrated in Table: 1. The difference in results is due to the bed geometry could not be reflected as exactly as the physical model. Various parameters like Manning's value, cell size and the system of geometry interpolation may cause the difference in velocity magnitude and water surface elevation. For model validation, velocity profile at only one cross-section was available i.e. at the inflow section which limits the accuracy in numerical modeling. So it is crucial to have more than one data for better validation.

Referring Fig: 18,Area I has higher field velocity which later shifted to Area II and Area III along with the reservoir drawdown. Shifting of higher field velocity contributes in achieving the riverine condition throughout a considerable length of time. And lowering of the reservoir water level forces sediment to move forming a flushing channel towards the outlet. The channel formation along with the time can be seen in Fig:19 for flushing with 500 m^3/sec. Similarly, velocity field relocation and channel formation is also observed in flushing with 1000 m^3/sec as in Fig: 21 and 22. The highest magnitude of velocity in 500 m^3/sec and 1000 m^3/sec is 4.4 m/s and 5.1 m/sec respectively.

The effectiveness of flushing of sediment through reservoir following the erosion and redeposition process depends on the water level in the reservoir and respective field velocity. When the water level in the reservoir is high (an initial condition in the present study), the water velocity is too low to excite the sediment movement in the reservoir. The velocity is high at the outlet section which erode sediment in that section only (Fig: 19). These velocities have negligible impacts on the upstream reservoir area to cause sediment erosion. So, proper reservoir drawdown is important for effective and efficient sediment flushing. When the reservoir is further drawdown and reached to intermediate level, water velocity increases at the upstream of the reservoir which further erodes the sediment, transporting toward the outlet section resulting in the erosion channel. At this stage channel will start to extend towards the upstream area of the reservoir as in Fig: 20(b). Similarly, the channel gets extended towards the upstream of Area II and deposition at the downstream bed. A similar pattern is observed in Area III near the spillway section. Later, when there is an extreme drawdown of reservoir reaching spillway crest level, development of scouring velocity occurs throughout the length of the reservoir. This will occur the retrogressive erosion of previously existing sediment with the development of deeper channel as compared to intermediate reservoir level drawdown.

The results from the numerical simulation are compared to the physical model on the basis of bed level change. Referring to flushing with 500 m^3/sec, the erosion and deposition pattern is well collated with the physical model expect in some areas like the left side of the bend of Area II and in front of the spillway section as shown in Fig: 20 (b and c). A

significant difference is observed in Area II for deposition. The simulated model reveals the increase in the deposition by 5 cm. The possible reason for deviation of result is due to adaptation of interpolated discharge hydrograph which generates the higher velocity at the bend section. After striking the water (with high-velocity field) with the bend, the velocity field gets dispersed as shown in Fig: 18(b) to dissipate the energy. In addition, it causes the backwater effect which increases the water level at control point 1, as illustrated in Fig: 17. This effects the wetting/drying algorithm which eventually has an impact on the flow direction resulting in the deposition of sediment on left side of bend as in Fig: 19(b), unlike in the physical model.

In Area III, the simulation results show higher erosion and deposition than Area II which is similar in the physical model. However, numerical modeling reflects overestimation of erosion at upstream part and different deposition patterns at downstream reaching near the spillway section. The physical model shows a narrow erosion channel located at the bend section, while simulation gives a wider erosion channel with a deeper part near to right side. During the free-flow condition, shallow depth can be found in Area III. As there is no complete formation of erosion channel, flow can be easily deflected in the presence of small disturbance which causes the deposition of sediment in a wider section as compared to the physical model. Comparison of change in volume of deposition and scouring after simulation shows similar values.

Moving towards flushing with 1000 m^3/sec, the scouring pattern is similar to physical model while the deposition is different. In simulated model high deposition of 15 cm approximately can be seen at the downstream bend of Area I(from Fig: 23) while no bed level changes occurs in physical model(as in Fig: 10). The reason behind this may be no enough development of high velocity to swipe off the deposited sediment after free flow condition. The less velocity in that section can be due to decrease in water surface elevation as Control Point 1 as shown in Fig: 24 which hinders the transportation of deposited sediments in all Area of interest. In case of Area II, the depth of erosion and deposition is similar to physical model, but a clear scouring channel cannot be obtained in simulated model. While in Area III, simulation overestimates the erosion at bend of upstream area. Only some area in left side of sediment delta is removed by the flushing as compared to physical model. While the deposition of sediment is similar to physical model i.e. nearly 13 cm. Simulation gives the unrealistic values of scouring and deposition volume i.e. 0.587 m^3 and 0.723 m^3 with the opposite trend as compared to physical model. The possible reason behind this may be the under development of high velocity field throughout the length of reservoir after free flow condition.

8 Conclusion and Recommendation

8.1 Conclusion

The REEF3D: SFLOW model reveals the good agreement in imitating the flow pattern and the surface velocities of the physical model. Some disparity in the flow pattern at the sidewall of boundary and island, vortex have been observed in an unwanted area. The simulated averaged velocity is higher than the measured velocity by 5 cm/sec. The sensitivity analysis with the roughness values is tested during the hydrodynamic validation.

The erosion and deposition pattern after flushing with 500 m^3/sec obtained from simulation is similar to that of the physical model. However, some differences are observed in a certain section, like on the bend of Area II and downstream of Area III. The erosion in Area I from numerical modeling is similar to that of the physical model but the deposition is sightly higher in the simulated model. The predicted erosion and deposition in Area III is overestimated than the physical model. The model also predicted high value to some extent in case of change in volume of bed level.

In case of flushing with 1000 m^3/sec the model fails to replicate the deposition and scouring pattern in Area II and III expect in Area I. The model also over predicted the scouring and deposition volume with opposite trend to physical model.

8.2 Recommendations

Aiming to improvise the result from the numerical model, several further works can be performed which are listed below:

1. In order to enhance the accuracy of numerical modeling, it is recommended to validate the simulation with different parameters like surface velocities and water surface elevations at different cross-sections.
2. The present study has used the constant discharge without sediment feeding for flushing purposes, the natural discharge hydrograph and sediment feeding rate can be implemented to get a better overview in the sediment transport process.
3. The bed load simulation has been carried out using Van Rijn formula; it is recommended to test the bedload transport sensitivity using other approaches available in REEF3D: SFLOW.
4. Due to time constraint sensitivity analysis regarding grid size, critical shear stress value is not performed in the present study. So, it recommended to check the model performance with different grid size and ctritical shear stress value.
5. Current version of REEF3D: SFLOW is based on uniform grid size throughout the domain which restricts the enhancement of grid in the area of interest. So, the implementation of a nested or unstructured grid would help to get a better result in the area of bend or around the obstacles in the flow path.

6. Current version of REEF3D: SFLOW supports the single sediment size in sediment simulation. For a better understanding of the scouring and deposition, it would better if the particle size distribution can be employed in numerical modeling.

References

Afzal, M. S. (2013). 3d numerical modelling of sediment transport under current and waves. Master's thesis, Institutt for bygg, anlegg og transport.

Afzal, M. S., Bihs, H., and Kumar, L. (2020). Computational fluid dynamics modeling of abutment scour under steady current using the level set method. *International Journal of Sediment Research*, 35(4):355–364.

Ahn, J. (2012). *Numerical modeling of reservoir sedimentation and flushing processes*. PhD thesis, Colorado State University.

Aksoy, H., Mahe, G., and Meddi, M. (2019). Modeling and practice of erosion and sediment transport under change.

Annandale, G. (2013). *Quenching the thirst: sustainable water supply and climate change*. CreateSpace Independent Publ. Platform.

Auel, C. and Boes, R. M. (2011). Sediment bypass tunnel design–review and outlook. *Dams and reservoirs under changing challenges*, 40312.

Berthelsen, P. A. and Faltinsen, O. M. (2008). A local directional ghost cell approach for incompressible viscous flow problems with irregular boundaries. *Journal of computational physics*, 227(9):4354–4397.

Biron, P. M., Robson, C., Lapointe, M. F., and Gaskin, S. J. (2004). Comparing different methods of bed shear stress estimates in simple and complex flow fields. *Earth Surface Processes and Landforms: The Journal of the British Geomorphological Research Group*, 29(11):1403–1415.

Chaudhary, H., Isaac, N., Tayade, S., and Bhosekar, V. (2019). Integrated 1d and 2d numerical model simulations for flushing of sediment from reservoirs. *ISH Journal of Hydraulic Engineering*, 25(1):19–27.

Committee, C. F. D. (1998). Guide: Guide for the verification and validation of computational fluid dynamics simulations (aiaa g-077-1998 (2002)).

Dey, S. (2014). *Fluvial hydrodynamics*. Springer.

El kadi Abderrezzak, K. and Paquier, A. (2009). One-dimensional numerical modeling of sediment transport and bed deformation in open channels. *Water Resources Research*, 45(5).

Falgout, R. D. and Yang, U. M. (2002). Hypre, high performance preconditioners: Users manual. Technical report, Technical report, Lawrence Livermore National Laboratory, 2006. Paper ....

icold (2021). World Register of Dams. `https://www.icold-cigb.org/GB/worldregister/generalsynthesis.asp`. Accessed: 2021-04-19.

iha (2021). Binga Reservoir Longitudinal Profile. https://www.hydropower.org/sediment-management-case-studies/philippines-binga. Accessed: 2021-06-19.

Jiang, G.-S. and Shu, C.-W. (1996). Efficient implementation of weighted eno schemes. *Journal of computational physics*, 126(1):202–228.

Kajishima, T. and Taira, K. (2017). Computational fluid dynamics. *Cham: Springer International Publishing*, (1).

Kamath, A. M. (2012). Calculation of wave forces on structures using reef3d. Master's thesis, Institutt for bygg, anlegg og transport.

Kim, W. and Choi, H. (2019). Immersed boundary methods for fluid-structure interaction: A review. *International Journal of Heat and Fluid Flow*, 75:301–309.

Kobus, H. (1984). Wasserbauliches versuchswesen.-2.

Kondolf, G. M. (1997). Profile: hungry water: effects of dams and gravel mining on river channels. *Environmental management*, 21(4):533–551.

Kraft, S., Wang, Y., and Oberlack, M. (2011). Large eddy simulation of sediment deformation in a turbulent flow by means of level-set method. *Journal of Hydraulic Engineering*, 137(11):1394–1405.

Lawrence, L. C. C. (2021). Parallel Computation. https://hpc.llnl.gov/training/tutorials/introduction-parallel-computing-tutorial. Accessed: 2021-04-21.

Lee, C. and Foster, G. (2013). Assessing the potential of reservoir outflow management to reduce sedimentation using continuous turbidity monitoring and reservoir modelling. *Hydrological Processes*, 27(10):1426–1439.

Lysne, D. K., Glover, B., Støle, H., and Tesaker, E. (2003). *Hydraulic design*. Norwegian University of Science and Technology, Department of Hydraulic and ....

Mahmood, K. (1987). Reservoir sedimentation-impact, extent and mitigation. *World Bank technical paper*, 71.

Mohammad, M. E., Al-Ansari, N., Knutsson, S., and Laue, J. (2020). A computational fluid dynamics simulation model of sediment deposition in a storage reservoir subject to water withdrawal. *Water*, 12(4).

Molinas, A. and Yang, C. T. (1986). *Computer program user's manual for GSTARS (generalized stream tube model for alluvial river simulation)*. US Department of Interior, Bureau of Reclamation, Engineering and Research ....

Morris, G. L. (2020). Classification of management alternatives to combat reservoir sedimentation. *Water*, 12(3):861.

Morris, G. L. and Fan, J. (1998). *Reservoir sedimentation handbook: design and management of dams, reservoirs, and watersheds for sustainable use*. McGraw Hill Professional.

Novák, P., Moffat, A., Nalluri, C., and Narayanan, R. (2017). *Hydraulic structures*. CRC Press.

Odnature (2021). Sediment Transport model. `https://www.odnature.naturalsciences.be/downloads/coherens/documentation/chapter7.pdf`. Accessed: 2021-04-21.

Olsen, N. R. B. (2012). Numerical modelling and hydraulics. *Online manuscript*.

Omnisci (2021). Parallel Computation. `https://www.omnisci.com/technical-glossary/parallel-computing`. Accessed: 2021-04-21.

Osher, S. and Sethian, J. A. (1988). Fronts propagating with curvature-dependent speed: Algorithms based on hamilton-jacobi formulations. *Journal of computational physics*, 79(1):12–49.

Phien, H. N. and Arbhabhirama, A. (1979). A statistical analysis of the sediment volume accumulated in reservoirs. *Journal of Hydrology*, 44(3-4):231–240.

Shu, C.-W. and Osher, S. (1988). Efficient implementation of essentially non-oscillatory shock-capturing schemes. *Journal of computational physics*, 77(2):439–471.

Smith, T. and O'Connor, B. (1977). A two-dimensional model for suspended sediment transport. In *IAHR-congress, Baden-Baden, West Germany*.

Sumi, T., Yoshimura, T., Asazaki, K., Kaku, M., Kashiwai, J., and Sato, T. (2015). Retrofitting and change in operation of cascade dams to facilitate sediment sluicing in the mimikawa river basin. In *Proc. 25th congress of ICOLD, Stavanger*.

Syvitski, J. P., Vörösmarty, C. J., Kettner, A. J., and Green, P. (2005). Impact of humans on the flux of terrestrial sediment to the global coastal ocean. *science*, 308(5720):376–380.

Tigrek, S. and Aras, T. (2011). *Reservoir sediment management*. CRC Press.

Van Rijn, L. (1989). The state of the art in sediment transport modeling, in sediment transport modeling. *American Society of Civil Engineers, New York*.

Vörösmarty, C. J., Meybeck, M., Fekete, B., Sharma, K., Green, P., and Syvitski, J. P. (2003). Anthropogenic sediment retention: major global impact from registered river impoundments. *Global and planetary change*, 39(1-2):169–190.

Wang, W., Martin, T., Kamath, A., and Bihs, H. (2020). An improved depth-averaged non-hydrostatic shallow water model with quadratic pressure approximation. *International Journal for Numerical Methods in Fluids*, 92(8):803–824.

Wiberg, P. L. and Dungan Smith, J. (1989). Model for calculating bed load transport of sediment. *Journal of hydraulic engineering*, 115(1):101–123.

Wilcock, P. R. (1996). Estimating local bed shear stress from velocity observations. *Water Resources Research*, 32(11):3361–3366.

A Master Thesis Agreement

NTNU

M.Sc. THESIS IN HYDRAULIC ENGINEERING

Candidate: Mr. Sabin Bhandari

Title: 2D numerical simulation of sediment flushing in a hydropower reservoir

1. Background

Solar energy, Wind energy, Thermal energy, Biomass, and Hydropower energy are examples of major renewable energy sources in the present century. Among these, the hydropower is of a great interest among the market players and developers. The reasons behind it are the generation of energy from abundantly available water resources, highest energy payback ratio and ability to respond quickly during peak demands. Consequently, hydropower has taken a remarkable position in the energy market being a sustainable source of energy.
However, many hydropower plants (HPP) are facing technical challenges, among one of them are sediments. Hydropower dams are altering the sediment balance of a river reach significantly and have consequently to cope with the consequences. These consequences are e.g. lifetime reduction due to sedimentation processes, risk of destruction of the headworks due to extreme flood events or high operation and maintenance costs due to abrasion of turbines and hydraulic structures.
The case study for the present study will be the Binga HPP. The reservoir of the Binga HPP is located in the Agno River in the northern part of the Philippines. The sedimentation of the Binga reservoir is heavy and the pivot point of the delta is approaching the intake as well as the spillway. The front slope of the delta is posing an increased threat to the intake as an underwater slide may send debris and mud to the intake under a hazardous event like a large flood or an earthquake.
The present study will investigate the technical possibilities to use a 2D numerical to flush sediment out of the reservoir during a drawdown operation. This operation is technically and numerically very demanding. From a technical point of it is important to evaluate and maximize the efficiency of the flushing. Flushing is very costly from the operational point of view and it is therefore very important to know the efficiency in advance. From the numerical point of view is the numerical simulation of the free surface during a flushing operation demanding. The model must be robust enough in order not to diverge and accurate enough to make reliable prognosis of the efficiency.

2. Work description

The thesis shall cover, though not necessarily be limited to the main tasks listed below.
Based on the available documentation the following shall be carried out:

1 Literature review on drawdown sediment flushing in terms of application range and efficiency.
2 Setting up the grid for the study case in a 2D hydrodynamic model.
3 Document the flow situation for 1000 m^3/s and compare it with the data of the physical model.
4 Run the numerical model for the flushing of 500 m^3/s and 1000 m^3/s and compare with the data obtained by the physical model.
5 Based on the results, suggest a strategy for the optimal flushing operation with respect to discharge.

NTNU

6 Discussion of the results
7 Conclusions
8 Proposals for future work
9 Prepare a 15 min presentation of the study and the main result

The literature review should outline the previous contributions in a condensed manner and result in the motivation for the current study.

3. Supervision

Prof. Nils Rüther will be the main supervisor. Postdoctoral researcher Behnam Balouchi and Associate Prof. Hans Bihs are appointed as co-supervisors. The supervisors shall assist the candidate and make relevant information, documents and data available.
Discussion with and input from other research or engineering staff at NTNU or other institutions are recommended. Significant inputs from others shall be referenced in a convenient manner.
The research and engineering work carried out by the candidate in connection with this thesis shall remain within an educational context. The candidate and the supervisors are free to introduce assumptions and limitations, which may be considered unrealistic or inappropriate in a contract research or a professional/commercial context.

4 Report format and submission

The report should be written with a text editing software. Figures, tables and photos shall be of high quality. The report format shall be in the style of scientific reports and must contain a summary, a table of content, and a list of references.

The report shall be submitted electronically in B5-format .pdf-file in Blackboard, and three paper copies should be handed in to the institute. Supplementary working files such as spreadsheets, numerical models, program scripts, figures and pictures shall be uploaded to Blackboard. The summary shall not exceed 450 words. The Master's thesis should be submitted within 15th of June 2021.

The candidate shall present the work at a MSc. seminar towards the end of the master period. The presentation shall be given with the use of powerpoint or similar presentation tools. The date and format for the MSc. seminar will be announced during the semester.

Trondheim, 15. January 2021

Nils Rüther
Professor
Department of Civil and Environmental Engineering
NTNU

B REEF3D: SFLOW Input Files

B.1 Input files for Hydrodynamic Simulation

Command used for hydrodynamic simulation(DIVEMESH: control.txt file)

C 11 21 # Boundary condition on surfaceside 1 as wall

C 12 21 # Boundary condition on surfaceside 2 as wall

C 13 21 # Boundary condition on surfaceside 3 as wall

C 14 21 # Boundary condition on surfaceside 4 as wall

C 15 21 # Boundary condition on surfaceside 5 as wall

C 16 3 # Boundary condition on surfaceside 6 as symmetry plane

B 1 0.05 # Grid size

B 10 684.3085 704.451 499.017 529.1637 -0.001 0.5 # rectangular domain

G 10 1 # turn on geodat

G 15 2 # interpolation scheme: local inverse distance interpolation

G 51 1 # automatic hole check and hole fill for incomplete geodata set

G 52 0.7 # base topography value for local inverse distance interpolation

G 53 0.5 # automatic search radius factor (times dx)

G 13 29 # rotation angle of geo coordinates around vertical axis

G 14 704.487 513.7330 # x-coordinate and y-coordinate of origin for the rotation angle of geo coordinates around vertical axis

M 10 4 # Number of processe

Command used for hydrdynamic simulation(REEF3D: ctrl.txt file)
B 50 0.0166 # Global wall roughness
B 60 0 # Enable ioFlow for open channel flow

F 50 4 # Fix Level Set for inflow or outflow: Fix None
F 60 0.305 # initial still water level for the whole domain

N 45 40000 # Maximum number of iteration
N 46 1000 # Maximum number of solver iterations
N 47 0.1 # Factor for CFL
N 61 500 # Stopping criteria for crtical velocities

M 10 4 # Number of processors
P 10 1 # Print paraview binary format
P 20 10 # Print results every ith iteration
W 10 0.0143 # Discharge
W 22 -9.81 # Acceleration due to Gravity, z-component

A 10 2 # Turn of SFLOW hydrodynamic model
A 209 0
A 210 3 # Time scheme for SFLOW momentum equations : 3rd-order Runge-Kutta
A 212 2 # Turn on diffusion for SFLOW velocities : OFF
A 211 4 # Convection scheme for SFLOW momentum equations : WENO FLUX
A 214 0 # Turn on convection for vertical SFLOW velocity ws : OFF
A 217 2 # Boundary conditions at walls : no-slip
A 218 1 # Turn on roughnes : ON
A 220 0 # Pressure scheme for SFLOW dynamics pressure ws: hydrostatic
A 240 1 # Free surface scheme for SFLOW: ON
A 243 1 # Turn on wetting and drying algorithm: ON
A 246 1 # Turn on breaking wave algorithm (turns off dynamics pressure for breaking waves): ON
A 260 3 # Turbulence model: Prandtl length scale mode
A 261 0.267 # Length scale factor for length scale turbulence model

B 440 1 2 687.477 688.357 523.0 529.164 # Boundary condition of inlet
B 411 1 -0.0286 # Discharge
b 413 1 0.32 # Waterlevel
b 418 1 1 # free stream flow

B 440 2 4 703.00 704.451 512.426 513.827 # Boundary condition of outlet
B 411 2 0.0286 # Discharge
B 413 2 0.305 # Waterlevel
b 418 2 1 # free stream flow

B.2 Input files for Sediment Simulation

Command used for sediment simulation(REEF3D ctrl.txt file)

```
B 60 1 # Enable ioFlow for open channel flow: Constant inflow

F 50 2 # Fix Level Set for inflow or outflow: Outflow Fixed
F 60 0.33 # initial water level

N 41 22100 # Maximum modeled time
N 46 100 # Maximum number of solver iterations
N 47 0.1 # Factor for CFL
N 48 1 # Adaptive timestepping: ON
N 61 1000 # Stopping criterion for critical velocities

M 10 4

P 10 1 # Print paraview binary format: ON
P 27 1 # Print topo to vtu file: ON
P 79 1 # print out bed shear stress to vtu file
P 30 600 # Print result every i^th second

B 440 1 2 685.268 687.995 523.0 527.036 # inlet face
B 421 1 1 # water level hydrograph: ON
B 422 1 1  # discharge level hydrograph: ON

B 440 1000 4 703.00 704.451 512.426 513.827   #oulet face 4
B 421 1000 1 # water level hydrograph: ON
B 422 1000 1  # discharge level hydrograph: ON

S 10 1 # sediment transport module : ON
S 11 1 # Bedload trasnport formuls : Van Rijn
S 14 0.1 # Factor of CFL for sediment transport module
S 15 0 # Sediment timestep selectio: adopted from S 14
S 16 1 3 # bed shear stress formulation: Wall function/velocity based
S 19 2210000 # Maximum modelled time for sediment
S 20 0.00027 # Sediment size d50
S 21 3.0 # Factor for d50 in calculation of ks in bedshear routine
S 22 2650.0 # Sediment density

S 30 0.047 # Shields parameter
S 50 4 # Exner equation discretization: WENO5 FLUX
```

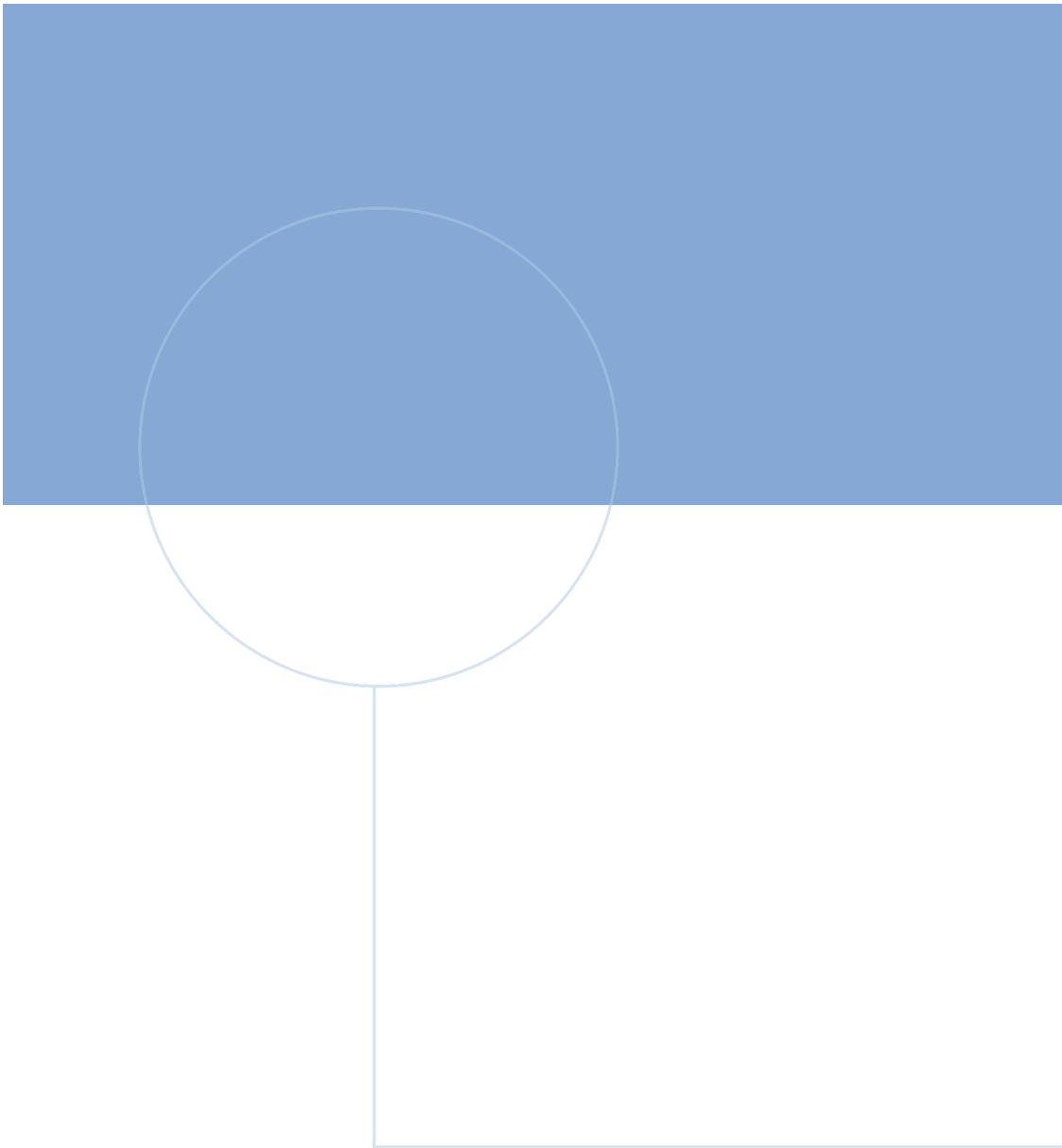

NTNU

Norwegian University of
Science and Technology